

# A LINEAR SECOND-ORDER MAXIMUM BOUND PRINCIPLE-PRESERVING BDF SCHEME FOR THE ALLEN-CAHN EQUATION WITH A GENERAL MOBILITY\*

DIANMING HOU<sup>1</sup>   LILI JU<sup>2</sup>   ZHONGHUA QIAO<sup>3</sup>

**ABSTRACT.** In this paper, we propose and analyze a linear second-order numerical method for solving the Allen-Cahn equation with a general mobility. The proposed fully-discrete scheme is carefully constructed based on the combination of first and second-order backward differentiation formulas with nonuniform time steps for temporal approximation and the central finite difference for spatial discretization. The discrete maximum bound principle is proved of the proposed scheme by using the kernel recombination technique under certain mild constraints on the time steps and the ratios of adjacent time step sizes. Furthermore, we rigorously derive the discrete  $H^1$  error estimate and energy stability for the classic constant mobility case and the  $L^\infty$  error estimate for the general mobility case. Various numerical experiments are also presented to validate the theoretical results and demonstrate the performance of the proposed method with a time adaptive strategy.

## 1. INTRODUCTION

In this paper, we consider the following Allen-Cahn equation with a general mobility:

$$\begin{cases} \frac{\partial \phi}{\partial t} = -M(\phi)\mu, & (\mathbf{x}, t) \in \Omega \times (0, T], \\ \mu = -\varepsilon^2 \Delta \phi + F'(\phi), & (\mathbf{x}, t) \in \Omega \times (0, T], \end{cases} \quad (1.1)$$

with the initial condition  $\phi(\mathbf{x}, 0) = \phi_0(\mathbf{x})$  for any  $\mathbf{x} \in \Omega$  and subject to the homogeneous Neumann or the periodic boundary condition, where  $\Omega$  is a bounded Lipschitz domain in  $\mathbb{R}^d$  ( $d = 1, 2, 3$ ),  $T > 0$  is the terminal time,  $\phi(\mathbf{x}, t)$  is the unknown function,  $\varepsilon > 0$  represents the interfacial

---

*Date:* March 3, 2023.

*2010 Mathematics Subject Classification.* 65M06, 65M15, 41A05, 41A25.

*Key words and phrases.* Allen-Cahn equation, general mobility, maximum bound principle, nonuniform time steps.

<sup>1</sup>School of Mathematics and Statistics, Jiangsu Normal University, Xuzhou, Jiangsu 221116, China. Email: dmhou@stu.xmu.edu.cn. Current address: Department of Applied Mathematics, The Hong Kong Polytechnic University, Hung Hom, Kowloon, Hong Kong. D. Hou's work is partially supported by Natural Science Foundation of China grant 12001248, Jiangsu Province Higher Education Institutions grant BK20201020, Jiangsu Province Universities Science Foundation grant 20KJB110013 and Hong Kong Polytechnic University grant 1-W00D.

<sup>2</sup>Department of Mathematics, University of South Carolina, Columbia, SC 29208, USA. Email: ju@math.sc.edu. L. Ju's work is partially supported by US National Science Foundation grant DMS-2109633.

<sup>3</sup>Department of Applied Mathematics, The Hong Kong Polytechnic University, Hung Hom, Kowloon, Hong Kong. Email: zqiao@polyu.edu.hk. Z. Qiao's work is partially supported by the Hong Kong Research Grants Council RFS grant RFS2021-5S03 and GRF grant 15302122, the Hong Kong Polytechnic University grant 4-ZZLS, and CAS AMSS-PolyU Joint Laboratory of Applied Mathematics.

width parameter,  $M(\phi) \geq 0$  is a general mobility function, and  $F(\phi) = \frac{1}{4}(1 - \phi^2)^2$  is the double-well potential function. This problem has a structure of  $L^2$  gradient flow corresponding to the following free energy functional  $E(\phi)$ , defined by

$$E(\phi) = \int_{\Omega} \left( \frac{\varepsilon^2}{2} |\nabla \phi|^2 + F(\phi) \right) d\mathbf{x}. \quad (1.2)$$

This structure implies that solution of (1.1) will approach to a steady state as  $t \rightarrow \infty$ , provided all steady states are isolated. It is a physically attractive and thermodynamically-consistent model often used to describe the transitions of the phases in the binary alloys. More specifically, the Allen-Cahn equation (1.1) satisfies the following energy dissipation law

$$\frac{d}{dt} E(\phi) = - \int_{\Omega} M(\phi) \mu^2 d\mathbf{x} \leq 0, \quad (1.3)$$

which indicates that the free energy  $E(\phi)$  monotonically decreases in time. Furthermore, the Allen-Cahn equation (1.1) satisfies the maximum bound principle (MBP), i.e.,  $|\phi(\mathbf{x}, t)| \leq 1$  if  $|\phi(\mathbf{x}, 0)| \leq 1$  for any  $\mathbf{x} \in \Omega$  and  $t \geq 0$ , and we refer to [46] for more discussions. The MBP and energy dissipation law are two important features of the equation (1.1), and thus it is highly desired for the numerical schemes to preserve these physical properties in the discrete level.

During the past decades, there have been extensive works devoted to the development of numerical methods for the Allen-Cahn equation (1.1) with preservation of discrete MBP and energy stability, especially for the constant mobility case. First-order (in time) linear stabilized schemes with central finite difference method for spatial discretization were obtained for the Allen-Cahn equation (1.1) with a constant mobility in [50] and the generalized Allen-Cahn equation with an advection term in [46], which are unconditionally energy stable and preserve the MBP simultaneously. A second-order convex splitting scheme based on Crank-Nicolson approach was investigated for fractional-in-space Allen-Cahn equation in [26], in which the discrete MBP and energy dissipation were rigorously established. However, it results in a nonlinear system to be solved at each time step. Hou et al. [25] developed a stabilized second-order Crank-Nicolson/Adams-Bashforth scheme for the Allen-Cahn equation, which preserves the discrete MBP and energy stability conditionally, and leads to solutions of only linear Poisson-type equations with constant coefficients at each time step. Recently, Cheng et al. [13, 14] proposed a Lagrange multiplier approach to construct positivity and bound preserving schemes for a class of semi-linear and quasi-linear parabolic equations. They have provided a new interpretation for the cut-off approach. Based on cut-off approach and the scalar auxiliary variable (SAV) method [1, 48], Yang et al. developed a class of arbitrarily high-order energy-stable and maximum bound preserving schemes for Allen-Cahn equation with a constant mobility in [56].

Du et al. developed first-order exponential time differencing (ETD) and second-order ETD Runge-Kutta (ETDRK2) schemes for the nonlocal Allen-Cahn equation, which preserves the discrete MBP unconditionally in [16], and later they also established an abstract framework on the MBP for a class of semilinear parabolic equations in [17]. These ETD approaches were also successfully applied to the conservative Allen-Cahn equations in [28, 34] of preserving the MBP and mass conservation in the discrete level, and the molecular beam epitaxial model [7, 11] of maintaining the discrete energy stability. Combining SAV technique with the stabilized first-order ETD and ETDRK2 methods, Ju et al. [29, 30] successfully constructed both the energy

dissipation law and the MBP preserving schemes for a class of Allen-Cahn type gradient flows. The unconditional energy stability of the stabilized ETDRK2 scheme for the gradient flows are also established in [18]. Based on integrating factor Runge-Kutta (IFRK) method, high-order MBP preserving schemes in time were recently developed for the semilinear parabolic equations in [31]. Subsequently, a family of stabilized IFRK schemes (up to the third-order and fourth-order) were proposed in [35, 57, 58] to preserve the discrete MBP unconditionally. Recently, an arbitrarily high-order multistep exponential integrator method was presented in [33] by enforcing the maximum bound via a cut-off operation. However, these high-order MBP-preserving ETD and IFRK methods seem difficultly to be extended to the problems with variable mobilities, since they are derived from either the variation-of-constant formula or an exponential transformation of the solution. We also would like to remark that all above MBP-preserving and energy stable scheme are based on the single time-stepping approach. There also exist few research and results on the MBP preservation of multiple time-stepping method, such as the popular high-order BDF schemes. Liao et al. studied the two-step second-order backward differentiation formula (BDF2) scheme for the time discretization of the Allen-Cahn equation with a constant mobility in [41], in which the MBP preservation and energy stability are established under certain mild constraints on the time steps and the ratios of adjacent time step sizes. However, it uses fully implicit treatment for the nonlinear term and thus leads to solving a nonlinear system at each time step. There also have been a lot of research work [6, 10, 12, 20, 36, 37, 44, 55] on high-order BDF schemes for gradient flows, which maintain certain discrete energy stability.

Another common feature of the Allen-Cahn equation (1.1) is that its evolution process often takes quite long time before it settles at a steady state. Moreover, it usually undergoes both fast and slow changing stages during the whole evolution process. Therefore, it is also highly useful to develop high-order structure-preserving numerical schemes with variable time steps for the Allen-Cahn equation, so that some existing time adaptive strategies can be easily applied. In this paper, we will propose and analyze an efficient linear second-order numerical method with nonuniform time steps for solving the Allen-Cahn equation with a general (constant or variable) mobility, which is based on the nonuniform BDF2 approach [4, 9, 23, 41] and preserves the discrete MBP under some mild constraints like [41].

The rest of the paper is organized as follows: In Section 2, we first review some preliminaries on the temporal and spatial discretization, and then propose the linear second-order BDF scheme for Allen-Cahn equation (1.1). Next we establish the discrete MBP of the proposed scheme using the kernel recombination technique in Section 3. In Section 4, some results on error estimates in the  $L^\infty$  and  $H^1$  norms and energy stability are rigorously derived. Several examples are tested in Section 5 to numerically validate the theoretical prediction and demonstrate the performance of the proposed scheme. Finally, some concluding remarks are drawn in section 6.

## 2. THE LINEAR SECOND-ORDER BDF SCHEME WITH NONUNIFORM TIME STEPS

We first briefly review the BDF2 formula for approximating time derivative and the central finite difference for discretizing the Laplacian, and then propose a linear second-order BDF scheme for the Allen-Cahn equation with a general mobility (1.1). Without loss of generality, we focus on the two-dimensional problem ( $d = 2$ ) with the homogenous Neumann boundary condition, i.e.,

$\frac{\partial \phi}{\partial \mathbf{n}}|_{\partial \Omega} = 0$  in what follows. It is easy to extend the corresponding results to the cases of higher dimensional spaces and/or the periodic boundary condition.

**2.1. The BDF2 formula with nonuniform time steps and its reformulation through kernel recombination.** Let  $\{\tau_n = t_n - t_{n-1} > 0\}_{n=1}^N$  denote the time step sizes of a general partition of the time interval  $[0, T]$  such that  $t_0 = 0$  and  $\sum_{n=1}^N \tau_n = T$ , and  $\{\gamma_{n+1} = \frac{\tau_{n+1}}{\tau_n} > 0\}_{n=1}^{N-1}$  denote the ratios of the corresponding two adjacent time step sizes. Define  $\tau = \max_{1 \leq n \leq N} \tau_n$  as the maximum time step size of such time partition and  $\gamma_{max} = \max_{1 \leq n \leq N} \gamma_n$  as the maximum adjacent time-step ratio.

For any function  $\phi(t)$  defined on  $[0, T]$ , denote  $\Pi_{2,n}\phi(t)$  as its quadratic interpolation operator using the three points  $(t_{n-1}, \phi(t_{n-1}))$ ,  $(t_n, \phi(t_n))$  and  $(t_{n+1}, \phi(t_{n+1}))$ , and we then have

$$\Pi_{2,n}\phi(t) = \phi(t_{n-1}) \frac{(t-t_n)(t-t_{n+1})}{\tau_n(\tau_n + \tau_{n+1})} - \phi(t_n) \frac{(t-t_{n-1})(t-t_{n+1})}{\tau_n \tau_{n+1}} + \phi(t_{n+1}) \frac{(t-t_{n-1})(t-t_n)}{(\tau_n + \tau_{n+1})\tau_{n+1}}$$

for any  $t \in [t_{n-1}, t_{n+1}]$  and consequently

$$\frac{\partial \Pi_{2,n}\phi}{\partial t}(t_{n+1}) = \frac{1}{\tau_{n+1}} \left( \frac{1+2\gamma_{n+1}}{1+\gamma_{n+1}} \phi(t_{n+1}) - (1+\gamma_{n+1})\phi(t_n) + \frac{\gamma_{n+1}^2}{1+\gamma_{n+1}} \phi(t_{n-1}) \right).$$

Thus the correspondingly derived second-order BDF approximation to  $\phi'(t)$  at  $t = t_{n+1}$  reads:

$$\begin{aligned} \phi'(t_{n+1}) &\approx F_2^{n+1}\phi = \frac{1}{\tau_{n+1}} \left( \frac{1+2\gamma_{n+1}}{1+\gamma_{n+1}} \phi^{n+1} - (1+\gamma_{n+1})\phi^n + \frac{\gamma_{n+1}^2}{1+\gamma_{n+1}} \phi^{n-1} \right) \\ &= b_0^n \delta_\tau \phi^{n+1} + b_1^n \delta_\tau \phi^n, \quad n = 1, 2, \dots, N-1, \end{aligned} \quad (2.1)$$

where  $\delta_\tau \phi^{n+1} = \phi^{n+1} - \phi^n$ ,  $\phi^n$  is a certain approximation to  $\phi(t_n)$ , and the discrete convolution kernels

$$b_0^n = \frac{1+2\gamma_{n+1}}{\tau_{n+1}(1+\gamma_{n+1})} > 0, \quad b_1^n = -\frac{\gamma_{n+1}^2}{\tau_{n+1}(1+\gamma_{n+1})} < 0.$$

For  $n = 0$ , if we set  $b_0^0 = 1/\tau_1$  and  $b_1^0 = 0$ , then  $F_2^1\phi = \frac{\delta_\tau \phi^1}{\tau_1}$  degrades to the first-order BDF approximation to  $\phi'(t)$  at  $t_1$ , i.e., the well-know backward Euler approximation

$$\phi'(t_{n+1}) \approx F_1^{n+1}\phi = \frac{\delta_\tau \phi^{n+1}}{\tau_{n+1}}, \quad n = 0, 1, \dots, N-1.$$

A novel technique through variable-weights recombination of a new specially-created variable was first proposed in [43] to achieve  $3 - \alpha$  order accuracy for the discrete form of  $\alpha$ -th order fractional Caputo derivative under the uniform time partition, in which the reformed convolution kernels are positive and monotone and play an important role in stability and convergence analysis. Also see [40, 41] for some recent developments in this direction. Following this kernel recombination technique, we define a new variable  $\psi$  as

$$\psi^{n+1} = \phi^{n+1} - \eta \phi^n, \quad n = 0, 1, \dots, N-1, \quad (2.2)$$

with  $\psi^0 = \phi^0$ , where  $\eta$  is a constant parameter to be determined such that the reformed discrete convolution kernels are positive and monotone. Then we have for  $n = 0, 1, \dots, N-1$ ,

$$\phi^{n+1} = \sum_{k=0}^{n+1} \eta^{n+1-k} \psi^k, \quad \delta_\tau \phi^{n+1} = \sum_{k=0}^n \eta^{n-k} \delta_\tau \psi^{k+1} + \eta^{n+1} \phi^0.$$

Combing (2.1) and the above identities, we can equivalently reform the BDF2 formula (2.1) as follows

$$F_2^{n+1}\phi = \sum_{k=0}^n d_{n-k}^n \delta_\tau \psi^{k+1} + d_{n+1}^n \psi^0, \quad 1 \leq n \leq N-1, \quad (2.3)$$

where the reformed discrete convolution kernels are defined by

$$d_0^n = b_0^n, \quad d_k^n = \eta^{k-1} (b_0^n \eta + b_1^n), \quad 1 \leq k \leq n+1. \quad (2.4)$$

Thus we have

$$d_{k+1}^n = \eta d_k^n, \quad 1 \leq k \leq n. \quad (2.5)$$

In order to make  $\{d_k^n\}_{k=0}^{n+1}$  positive and decreasing, i.e.,  $d_0^n \geq d_1^n \geq \dots \geq d_{n+1}^n \geq 0$ , we need to require  $\eta$  to satisfy that

$$0 < \frac{\gamma_{n+1}^2}{1 + 2\gamma_{n+1}} = -\frac{b_1^n}{b_0^n} \leq \eta < 1$$

for all  $n = 1, 2, \dots, N-1$ . Since  $0 < \gamma_{n+1} \leq \gamma_{max}$  and  $\frac{x^2}{1+2x}$  is increasing in  $(0, +\infty)$ , we then have

$$\frac{\gamma_{max}^2}{1 + 2\gamma_{max}} \leq \eta < 1, \quad (2.6)$$

which also implies  $0 < \gamma_{max} < 1 + \sqrt{2}$ .

**2.2. The central finite difference for the Laplacian.** We firstly recall some notations and results of the discrete function spaces and operators from [2, 3, 27, 38, 47, 51, 52, 54]. Let  $\Omega = (0, L_x) \times (0, L_y)$ , and we also assume  $L_x = L_y = L$  and the spatial grid spacing  $h = L/M$  for simplicity. We first define the following two finite grid sets:

$$\mathbf{E} = \{x_{i+\frac{1}{2}} = ih \mid i = 0, 1, \dots, M\}, \quad \mathbf{C} = \{x_i = (i - \frac{1}{2})h \mid i = 1, \dots, M\},$$

and then we introduce the following discrete function spaces:

$$\begin{aligned} \mathcal{C}_h &= \{U : \mathbf{C} \times \mathbf{C} \rightarrow \mathbb{R} \mid U_{i,j}, 1 \leq i, j \leq M\}, \\ e_h^x &= \{U : \mathbf{E} \times \mathbf{C} \rightarrow \mathbb{R} \mid U_{i+\frac{1}{2},j}, 0 \leq i \leq M, 1 \leq j \leq M\}, \\ e_h^y &= \{U : \mathbf{C} \times \mathbf{E} \rightarrow \mathbb{R} \mid U_{i,j+\frac{1}{2}}, 1 \leq i \leq M, 0 \leq j \leq M\}, \\ e_{0,h}^x &= \{U \in e_h^x \mid U_{\frac{1}{2},j} = U_{M+\frac{1}{2},j} = 0, 1 \leq j \leq M\}, \\ e_{0,h}^y &= \{U \in e_h^y \mid U_{i,\frac{1}{2}} = U_{i,M+\frac{1}{2}} = 0, 1 \leq i \leq M\}. \end{aligned}$$

Under the homogeneous Neumann boundary condition, the discrete gradient operator  $\nabla_h = (\nabla_h^x, \nabla_h^y) : \mathcal{C}_h \rightarrow (e_{0,h}^x, e_{0,h}^y)$  is defined by

$$(\nabla_h^x U)_{i+\frac{1}{2},j} = \frac{U_{i+1,j} - U_{i,j}}{h}, \quad 1 \leq i \leq M-1, 1 \leq j \leq M, \quad (2.7)$$

$$(\nabla_h^y U)_{i,j+\frac{1}{2}} = \frac{U_{i,j+1} - U_{i,j}}{h}, \quad 1 \leq i \leq M, 1 \leq j \leq M-1 \quad (2.8)$$

for any  $U \in \mathcal{C}_h$ , and the discrete divergence operator  $\nabla_h \cdot : (e_h^x, e_h^y) \rightarrow \mathcal{C}_h$  is represented by

$$(\nabla_h \cdot (U^x, U^y)^T)_{i,j} = \frac{U_{i+1/2,j}^x - U_{i-1/2,j}^x}{h} + \frac{U_{i,j+1/2}^y - U_{i,j-1/2}^y}{h}, \quad 1 \leq i, j \leq M \quad (2.9)$$

for any  $(U^x, U^y)^T \in (e_h^x, e_h^y)$ . Then the discrete Laplacian  $\Delta_h : \mathcal{C}_h \rightarrow \mathcal{C}_h$  by the central finite difference is defined by

$$(\Delta_h U)_{i,j} = (\nabla_h \cdot (\nabla_h U))_{i,j}, \quad 1 \leq i, j \leq M.$$

The two average operators  $a_x : e_h^x \rightarrow \mathcal{C}_h$  and  $a_y : e_h^y \rightarrow \mathcal{C}_h$  are defined by

$$(a_x U)_{i,j} = \frac{1}{2}(U_{i+\frac{1}{2},j} + U_{i-\frac{1}{2},j}), \quad 1 \leq i, j \leq M,$$

and

$$(a_y U)_{i,j} = \frac{1}{2}(U_{i,j+\frac{1}{2}} + U_{i,j-\frac{1}{2}}), \quad 1 \leq i, j \leq M$$

for any  $U \in e_h^y$ . We define some related discrete inner-products as follows:

$$\begin{aligned} \langle U, V \rangle_\Omega &= h^2 \sum_{i,j=1}^M U_{i,j} V_{i,j}, \quad \forall U, V \in \mathcal{C}_h, \\ [U^x, V^x]_x &= \langle a_x(U^x V^x), 1 \rangle_\Omega, \quad \forall U^x, V^x \in e_h^x, \\ [U^y, V^y]_y &= \langle a_y(U^y V^y), 1 \rangle_\Omega, \quad \forall U^y, V^y \in e_h^y, \\ [(U^x, U^y)^T, (V^x, V^y)^T]_\Omega &= [U^x, V^x]_x + [U^y, V^y]_y. \end{aligned}$$

Then we have the following result for the discrete analogue of integration by parts.

**Lemma 2.1** ([38, 51]). *For any  $U, V \in \mathcal{C}_h$ , it holds*

$$-\langle \Delta_h U, V \rangle_\Omega = [\nabla_h U, \nabla_h V]_\Omega.$$

For any  $U \in \mathcal{C}_h$ , we define the following discrete  $L^2$ ,  $H^1$  and  $L^\infty$  norms/semi-norms:

$$\begin{aligned} \|U\|_h^2 &= \langle U, U \rangle_\Omega, \\ \|\nabla_h U\|_h^2 &= [\nabla_h U, \nabla_h U]_\Omega = [d_x U, d_x U]_x + [d_y U, d_y U]_y, \\ \|U\|_{H_h^1}^2 &= \|U\|_h^2 + \|\nabla_h U\|_h^2, \quad \|U\|_\infty = \max_{1 \leq i \leq M} \sum_{j=1}^M |U_{i,j}| \end{aligned}$$

For convenience of description, we also define  $\vec{U} \in \mathbb{R}^{M^2}$  as the vector representation of  $U \in \mathcal{C}_h$ , in which the elements are arranged first along the  $x$ -direction then along the  $y$ -direction. Note that we do not differ them in places there is no ambiguity.

**2.3. The linear second-order BDF scheme for the Allen-Cahn equation.** Denote by  $\Pi_{\mathcal{C}_h}$  the operator pointwisely limiting a function onto  $\mathcal{C}_h$ . Let us first recall the fully-discrete linear first-order BDF scheme (called ‘‘BDF1’’) proposed in [46, 50] for solving the Allen-Cahn equation with a general mobility (1.1): given  $\Phi^0 = \Pi_{\mathcal{C}_h} \phi_0$ , for  $n = 0, 1, \dots, N-1$ , find  $\Phi^{n+1} \in \mathcal{C}_h$  such that

$$F_1^{n+1} \Phi - \varepsilon^2 M(\Phi^n) \Delta_h \Phi^{n+1} + f(\Phi^n) + S(\Phi^{n+1} - \Phi^n) = 0, \quad (2.10)$$

where  $F_1^{n+1} \Phi = \frac{\Phi^{n+1} - \Phi^n}{\tau_{n+1}}$  and  $f(\phi) = M(\phi)F'(\phi)$  and  $S \geq 0$  is a constant stabilizing parameter. We will denote the scheme (2.10) as  $\Phi^{n+1} = \text{BDF1}(\Phi^n, \tau_{n+1})$ . The above linear BDF1 scheme (2.10) also be rewritten in the following vector form:

$$F_1^{n+1} \vec{\Phi} - \varepsilon^2 \Lambda^n D_h \vec{\Phi}^{n+1} + f(\vec{\Phi}^n) + S(\vec{\Phi}^{n+1} - \vec{\Phi}^n) = 0, \quad (2.11)$$

where  $D_h = I \otimes G + G \otimes I \in \mathbb{R}^{M^2 \times M^2}$  with  $I$  denoting the identity matrix (with the matched dimensions) and

$$G = \frac{1}{h^2} \begin{pmatrix} -1 & 1 & & & & \\ 1 & -2 & 1 & & & \\ & \ddots & \ddots & \ddots & & \\ & & & 1 & -2 & 1 \\ & & & & 1 & -1 \end{pmatrix}_{M \times M},$$

and  $f(\vec{\Phi}^n) = \Lambda^n((\vec{\Phi}^n)^3 + \vec{\Phi}^n)$  is defined elementwise with the diagonal matrix  $\Lambda^n = \text{diag}(M(\vec{\Phi}^n))$ . Clearly,  $D_h$  is the corresponding matrix representation of  $\Delta_h$ .

In analogous to the energy  $E(\phi)$  defined in (1.2), we define the discrete energy  $E_h(\vec{\Phi}^n)$  as

$$E_h(\vec{\Phi}^n) = -h^2 \frac{\varepsilon^2}{2} (\vec{\Phi}^n)^T D_h \vec{\Phi}^n + h^2 \sum_{i=1}^{M^2} F(\vec{\Phi}_i^n) = \frac{\varepsilon^2}{2} [\nabla_h \Phi^n, \nabla_h \Phi^n]_\Omega + \langle F(\Phi^n), 1 \rangle_\Omega. \quad (2.12)$$

Then the unconditional energy stability and the discrete maximum bound principle of the fully-discrete BDF1 scheme (2.10) hold as stated in the following lemma, and we refer to Theorem 3.2 in [46] and Theorem 3 in [50] for details.

**Lemma 2.2** ([46, 50]). *Assume that  $\|\vec{\Phi}^0\|_\infty \leq 1$  and the stabilizing parameter*

$$S \geq \max_{\rho \in [-1, 1]} (M'(\rho)F'(\rho) + M(\rho)F''(\rho)), \quad (2.13)$$

*then it unconditionally holds for the BDF1 scheme (2.10) that  $\|\vec{\Phi}^{n+1}\|_\infty \leq 1$  for  $n = 0, 1, \dots, N-1$ . Particularly, if the mobility function  $M(\phi) \equiv 1$ , then*

$$E_h(\vec{\Phi}^{n+1}) \leq E_h(\vec{\Phi}^n) \quad (2.14)$$

*for all  $n = 0, 1, \dots, N-1$ , provided that  $S \geq 2$ .*

Now we are ready to construct a fully-discrete linear second-order BDF scheme with nonuniform time steps (called ‘‘BDF2’’ hereafter) for the Allen-Cahn equation with a general mobility (1.1) under the homogenous Neumann boundary condition: given  $\Phi^0 = \Pi_{\mathcal{C}_h} \phi_0$ , compute  $\Phi^1 = \text{BDF1}(\phi^0, \tau_1)$  and for  $n = 1, 2, \dots, N-1$ , find  $\Phi^{n+1} \in \mathcal{C}_h$  such that

$$\begin{cases} \Phi^{*,n+1} = \text{BDF1}(\Phi^n, \tau_{n+1}), & (2.15a) \end{cases}$$

$$\begin{cases} F_2^{n+1} \Phi - \varepsilon^2 M(\Phi^{*,n+1}) \Delta_h \Phi^{n+1} + f(\Phi^{*,n+1}) + S(\Phi^{n+1} - \Phi^{*,n+1}) = 0, & (2.15b) \end{cases}$$

where  $F_2^{n+1} \Phi = b_0^n (\Phi^{n+1} - \Phi^n) + b_1^n (\Phi^n - \Phi^{n-1})$ . We denote the scheme (2.15) as  $\phi^{n+1} = \text{BDF2}(\phi^n, \phi^{n-1}, \tau_{n+1}, \tau_n)$ . The above linear BDF2 scheme (2.15) can be rewritten in the following vector form:

$$\begin{cases} \vec{\Phi}^{*,n+1} = \text{BDF1}(\vec{\Phi}^n, \tau_{n+1}), & (2.16a) \end{cases}$$

$$\begin{cases} F_2^{n+1} \vec{\Phi} - \varepsilon^2 \Lambda^{*,n+1} D_h \vec{\Phi}^{n+1} + f(\vec{\Phi}^{*,n+1}) + S(\vec{\Phi}^{n+1} - \vec{\Phi}^{*,n+1}) = 0, & (2.16b) \end{cases}$$

where  $\Lambda^{*,n+1} = \text{diag}(M(\vec{\Phi}^{*,n+1}))$ .

## 3. THE DISCRETE MAXIMUM BOUND PRINCIPLE

In this section, we will prove the discrete maximum bound principle of the proposed BDF2 scheme (2.15) using the kernel recombination technique described in Section 2.1. Define  $\vec{\Psi}^n = \vec{\Phi}^n - \eta \vec{\Phi}^{n-1}$ , and then we can combine (2.2) and (2.3) to obtain the following kernel recombination form for (2.16b): for  $n = 1, 2, \dots, N-1$ ,

$$\left( (d_0^n + S)I - \varepsilon^2 \Lambda^{*,n+1} D_h \right) \vec{\Phi}^{n+1} = \eta d_0^n \vec{\Phi}^n + \sum_{k=0}^n (d_{n-k}^n - d_{n-k+1}^n) \vec{\Psi}^k + S \vec{\Phi}^{*,n+1} - f(\vec{\Phi}^{*,n+1}). \quad (3.1)$$

Substituting  $\vec{\Phi}^{n+1} = \sum_{k=0}^{n+1} \eta^{n+1-k} \vec{\Psi}^k$  into (3.1) yields

$$\left( (d_0^n + S)I - \varepsilon^2 \Lambda^{*,n+1} D_h \right) \vec{\Psi}^{n+1} = \sum_{k=0}^n Q_{n-k}^n \vec{\Psi}^k + S \vec{\Phi}^{*,n+1} - f(\vec{\Phi}^{*,n+1}), \quad (3.2)$$

where

$$Q_k^n = (d_k^n - d_{k+1}^n - S\eta^{k+1})I + \eta^{k+1} \varepsilon^2 \Lambda^{*,n+1} D_h, \quad 0 \leq k \leq n. \quad (3.3)$$

The following result for the estimation of  $Q_k^n$  holds (we also refer to Lemma 4.1 in [41] which is only for the specific case  $M(\phi) \equiv 1$ ).

**Lemma 3.1.** *Let  $n$  be any fixed integer such that  $1 \leq n \leq N-1$  and suppose  $\|\vec{\Phi}^{*,n+1}\|_\infty \leq 1$ . Assume that  $0 < \gamma_{n+1} < 1 + \sqrt{2}$ , the parameter  $\eta$  satisfies (2.6), and*

$$\tau_{n+1} \leq \frac{g(\gamma_{n+1}, \eta)}{S + 4L\varepsilon^2/h^2}, \quad (3.4)$$

where  $L = \max_{\rho \in [-1, 1]} M(\rho)$  and

$$g(s, z) = \frac{(1-z)((1+2s)z - s^2)}{z^2(1+s)}, \quad s \in (0, \gamma_{max}], \quad z \in \left[ \frac{\gamma_{max}^2}{1+2\gamma_{max}}, 1 \right).$$

Then it holds

$$\|Q_k^n\|_\infty \leq d_k^n - d_{k+1}^n - S\eta^{k+1}, \quad \forall 0 \leq k \leq n. \quad (3.5)$$

*Proof.* From the definition of  $Q_k^n$  in (3.3) and (2.4), it follows

$$\begin{aligned} Q_k^n &= (\eta^{k-1}(b_0^n \eta + b_1^n) - \eta^k(b_0^n \eta + b_1^n) - S\eta^{k+1})I + \eta^{k+1} \varepsilon^2 \Lambda^{*,n+1} D_h, \\ &= \eta^{k+1} \left( (\eta^{-2}(1-\eta)(b_0^n \eta + b_1^n) - S)I + \varepsilon^2 \Lambda^{*,n+1} D_h \right) \\ &= \eta^{k+1} \left( \left( \frac{g(\gamma_{n+1}, \eta)}{\tau_{n+1}} - S \right) I + \varepsilon^2 \Lambda^{*,n+1} D_h \right), \quad 1 \leq k \leq n, \end{aligned}$$

which means that all the entries of  $Q_k^n$  are nonnegative based on the definition of  $D_h$ , the fact of  $\|\Lambda^{*,n+1}\|_\infty \leq L$ , and (3.4). Thus we deduce that

$$\|Q_k^n\|_\infty = \max_{1 \leq i \leq M^2} \sum_{j=1}^{M^2} (Q_k^n)_{i,j} \leq d_k^n - d_{k+1}^n - S\eta^{k+1}, \quad \forall 1 \leq k \leq n,$$

by using the fact  $\sum_{j=1}^{M^2} (\Lambda^{*,n+1} D_h)_{i,j} = 0$  for any  $1 \leq i \leq M^2$ .



For the case of  $k = 0$ , using (2.4) and (3.4), we get

$$\begin{aligned} Q_0^n &= (d_0^n - d_1^n - S\eta)I + \eta\varepsilon^2\Lambda^{*,n+1}D_h \\ &= (b_0^n - b_0^n\eta - b_1^n - S\eta)I + \eta\varepsilon^2\Lambda^{*,n+1}D_h \\ &= \eta((\eta^{-2}(b_0^n\eta + b_1^n - b_0^n\eta^2 - b_1^n\eta) - \eta^{-2}b_1^n - S)I + \varepsilon^2\Lambda^{*,n+1}D_h) \\ &\geq \eta((\eta^{-2}(1 - \eta)(b_0^n\eta + b_1^n) - S)I + \varepsilon^2\Lambda^{*,n+1}D_h), \end{aligned}$$

which means that all the entries of  $Q_0^n$  are also nonnegative and consequently we obtain  $\|Q_0^n\|_\infty \leq d_0^n - d_1^n - S\eta$  by similar arguments as above.  $\square$

This lemma plays an important role in deriving the MBP property of the BDF2 scheme (2.15). We also remark that the inequality (3.4) doesn't explicitly give a principle for determining the range of feasible time step size  $\tau_{n+1}$  in practice, since  $\gamma_{n+1}$  in the righthand side of (3.4) depends on  $\tau_{n+1}$ . Next we drive a uniform upper bound for the time step size  $\tau_{n+1}$  independent on  $\gamma_{n+1}$  such that the estimate (3.5) for the matrix  $Q_k^n$  holds. In the numerical simulations, one can always set a pre-determined maximum adjacent time-step ratio  $\gamma_*$  such that  $\gamma_{n+1} \leq \gamma_*$  for all  $n \geq 1$ . Since it is required that  $0 < \gamma_{n+1} < 1 + \sqrt{2}$  (see Section 2.1), we choose  $\gamma_*$  from  $[1, 1 + \sqrt{2})$ . Noting that

$$\frac{\partial g}{\partial s}(s, z) = \frac{(1-z)(-s^2 - 2s + z)}{z^2(1+s)^2}, \quad s \in (0, \gamma_*], \quad z \in \left[\frac{\gamma_*^2}{1+2\gamma_*}, 1\right),$$

and combining with  $\sqrt{1+z} - 1 < \sqrt{2} - 1 < 1 \leq \gamma_*$ , it can be verified that for any fixed  $z$ ,  $g(s, z)$  is increasing in  $(0, \sqrt{1+z} - 1)$  and decreasing in  $(\sqrt{1+z} - 1, \gamma_*)$  with respect to  $s$ . Furthermore, since  $g(0, z) = \frac{1-z}{z} > \frac{(1-z)(3z-1)}{2z^2} = g(1, z) \geq g(\gamma_*, z)$  for  $z \in \left[\frac{\gamma_*^2}{1+2\gamma_*}, 1\right)$ , we have

$$g(\gamma_*, z) \leq g(\gamma_{n+1}, z)$$

for all  $\gamma_{n+1} \in (0, \gamma_*)$  and  $z \in \left[\frac{\gamma_*^2}{1+2\gamma_*}, 1\right)$ . Thus, it follows from Lemma 3.1 that the estimate (3.5) for the matrix  $Q_k^n$  holds for  $0 < \gamma_{n+1} \leq \gamma_* < 1 + \sqrt{2}$ , and

$$\tau_{n+1} \leq \frac{g(\gamma_*, \eta)}{S + 4L\varepsilon^2/h^2}, \quad \forall \eta \in \left[\frac{\gamma_*^2}{1+2\gamma_*}, 1\right). \quad (3.6)$$

Taking the fact

$$\frac{\partial g}{\partial \eta}(\gamma_*, \eta) = \frac{2\gamma_*^2 - (1 + \gamma_*)^2\eta}{(1 + \gamma_*)\eta^3},$$

together with  $\frac{\gamma_*^2}{1+2\gamma_*} < \frac{2\gamma_*^2}{(1+\gamma_*)^2} < 1$ , we see that  $g(\gamma_*, \eta)$  is increasing in  $(\frac{\gamma_*^2}{1+2\gamma_*}, \frac{2\gamma_*^2}{(1+\gamma_*)^2})$  and decreasing in  $(\frac{2\gamma_*^2}{(1+\gamma_*)^2}, 1)$  with respect to  $\eta$ . Thus, the optimal value of  $\eta$  for (3.6) is

$$\eta_* = \frac{2\gamma_*^2}{(1 + \gamma_*)^2}. \quad (3.7)$$

Summarizing the above discussions, we obtain the following result.

**Lemma 3.2.** *Let  $n$  be any fixed integer such that  $1 \leq n \leq N - 1$  and suppose  $\|\vec{\Phi}^{*,n+1}\|_\infty \leq 1$ . Assume that  $0 < \gamma_{n+1} \leq \gamma_* < 1 + \sqrt{2}$ ,  $\eta = \eta_*$ , and the time step size  $\tau_{n+1}$  satisfies*

$$\tau_{n+1} \leq \frac{\mathcal{G}(\gamma_*)}{S + 4L\varepsilon^2/h^2} \quad (3.8)$$

with

$$\mathcal{G}(\gamma_*) = g\left(\gamma_*, \frac{2\gamma_*^2}{(1+\gamma_*)^2}\right) = \frac{(1+2\gamma_* - \gamma_*^2)^2}{4\gamma_*^2(1+\gamma_*)}.$$

Then it holds

$$\|Q_k^n\|_\infty \leq d_k^n - d_{k+1}^n - S\eta_*^{k+1}, \quad \forall 0 \leq k \leq n. \quad (3.9)$$

**Remark 3.1.** Note that  $\mathcal{G}(\gamma_*)$  is decreasing with respect to  $\gamma_* \in (1, 1 + \sqrt{2})$ . Especially, we have  $\mathcal{G}(1) = \frac{1}{2}$  for the case of uniform time steps ( $\gamma_* = 1$ ), and  $\mathcal{G}(2) = \frac{1}{48}$  for the case of  $\gamma_* = 2$ .

In what follows, by default we always set  $\eta = \eta_*$  which is defined in (3.7). We next state the following useful lemmas.

**Lemma 3.3** ([26, 41, 50]). Suppose  $B = (b_{i,j})$  is a real  $P \times P$  matrix satisfying

$$b_{i,i} < 0, \quad |b_{i,i}| \geq \max_{1 \leq i \leq P} \sum_{j \neq i}^P |b_{i,j}|.$$

Let  $A = aI - B$  where  $a > 0$  is a constant, then

$$\|A\vec{U}\|_\infty \geq a\|\vec{U}\|_\infty, \quad \forall \vec{U} \in \mathbb{R}^P.$$

**Lemma 3.4** ([50]). If the stabilizing parameter  $S$  satisfies (2.13), then

$$|S\rho - f(\rho)| \leq S, \quad \forall \rho \in [-1, 1]. \quad (3.10)$$

*Proof.* Let  $h(\rho) = S\rho - f(\rho)$ . From (2.13), we have

$$h'(\rho) = S - [M'(\rho)F'(\rho) + M(\rho)F''(\rho)] \geq 0, \quad \forall \rho \in [-1, 1].$$

Together with  $h(-1) = -S$  and  $h(1) = S$ , we obtain (3.10).  $\square$

Now, we are ready to show the MBP of the BDF2 scheme (2.15).

**Theorem 3.1.** Assume that the stabilizing parameter  $S$  satisfies (2.13) and  $0 < \gamma_{n+1} \leq \gamma_* < 1 + \sqrt{2}$  for all  $1 \leq n \leq N - 1$ . In addition, assume that

$$\tau_1 \leq \frac{1 - \eta_*}{\eta_*(S + 4L\varepsilon^2/h^2)}, \quad (3.11)$$

and  $\tau_{n+1}$  satisfies (3.8) for  $n = 1, 2, \dots, N - 1$ . If  $\|\vec{\Phi}^0\|_\infty \leq 1$ , then it holds for the BDF2 scheme (2.15) that  $\|\vec{\Phi}^{n+1}\|_\infty \leq 1$  for  $n = 0, 1, \dots, N - 1$ .

*Proof.* For the first step, i.e.,  $\vec{\Phi}^1 = \text{BDF1}(\vec{\Phi}^0, \tau_1)$  when  $n = 0$ , it follows directly from Lemma 2.2 that  $\|\vec{\Phi}^1\|_\infty \leq 1$ . Substituting  $\vec{\Phi}^1 = \vec{\Psi}^1 + \eta_*\vec{\Phi}^0$  into (2.10) gives

$$\left(\left(\frac{1}{\tau_1} + S\right)I - \varepsilon^2\Lambda^0 D_h\right)\vec{\Psi}^1 = \left(\left(\frac{1 - \eta_*}{\tau_1} - \eta_*S\right)I + \eta_*\varepsilon^2\Lambda^0 D_h\right)\vec{\Psi}^0 + S\vec{\Phi}^0 - f(\vec{\Phi}^0). \quad (3.12)$$

Noting the constraint (3.11) together with the definition of  $D_h$  and a similar analysis used in Lemma 3.1, we derive that

$$\left(\left(\frac{1 - \eta_*}{\tau_1} - \eta_*S\right)I + \eta_*\varepsilon^2\Lambda^0 D_h\right)_{i,j} \geq 0, \quad 1 \leq i, j \leq M^2,$$

and consequently

$$\left\|\left(\frac{1 - \eta_*}{\tau_1} - \eta_*S\right)I + \eta_*\varepsilon^2\Lambda^0 D_h\right\|_\infty \leq \frac{1 - \eta_*}{\tau_1} - \eta_*S. \quad (3.13)$$

From (3.12), (3.13) and Lemma 3.3, it follows that

$$\begin{aligned}
\left(\frac{1}{\tau_1} + S\right)\|\vec{\Psi}^1\|_\infty &\leq \left\| \left( \left( \frac{1}{\tau_1} + S \right) I - \varepsilon^2 \Lambda^0 D_h \right) \vec{\Psi}^1 \right\|_\infty \\
&\leq \left\| \left( \left( \frac{1-\eta_*}{\tau_1} - \eta_* S \right) I + \eta_* \varepsilon^2 \Lambda^0 D_h \right) \vec{\Psi}^0 \right\|_\infty + \|S\vec{\Phi}^0 - f(\vec{\Phi}^0)\|_\infty \\
&\leq \left( \frac{1-\eta_*}{\tau_1} - \eta_* S \right) + S \\
&= \left( \frac{1}{\tau_1} + S \right) (1 - \eta_*),
\end{aligned}$$

where we have used Lemma 3.4. Thus we have  $\|\vec{\Psi}^1\|_\infty \leq 1 - \eta_*$ .

Next, for any  $1 \leq n \leq N - 1$ , we assume  $\|\vec{\Phi}^k\|_\infty \leq 1$  and  $\|\vec{\Psi}^k\|_\infty \leq 1 - \eta_*$  for  $1 \leq k \leq n$ . Using  $\vec{\Phi}^{*,n+1} = \text{BDF1}(\vec{\Phi}^n, \tau_{n+1})$ ,  $\|\vec{\Phi}^n\|_\infty \leq 1$ , and Lemma 2.2, we obtain  $\|\vec{\Phi}^{*,n+1}\|_\infty \leq 1$ . Thus, together with (3.1), (2.5) and Lemmas 3.3 and 3.4, we have

$$\begin{aligned}
(d_0^n + S)\|\vec{\Phi}^{n+1}\|_\infty &\leq \|((d_0^n + S)I - \varepsilon^2 \Lambda^{*,n+1} D_h) \vec{\Phi}^{n+1}\|_\infty \\
&\leq \eta_* d_0^n \|\vec{\Phi}^n\|_\infty + \sum_{k=0}^n (d_{n-k}^n - d_{n-k+1}^n) \|\vec{\Psi}^k\|_\infty + \|S\vec{\Phi}^{*,n+1} - f(\vec{\Phi}^{*,n+1})\|_\infty \\
&\leq \eta_* d_0^n + \sum_{k=1}^n (d_{n-k}^n - d_{n-k+1}^n) (1 - \eta_*) + (d_n^n - d_{n+1}^n) + S \\
&= \eta_* d_0^n + (d_0^n - d_n^n) (1 - \eta_*) + (1 - \eta_*) d_n^n + S \\
&= d_0^n + S,
\end{aligned}$$

which gives  $\|\vec{\Phi}^{n+1}\|_\infty \leq 1$ . Using (3.2) together with (2.5), Lemmas 3.2, 3.3 and 3.4, we get

$$\begin{aligned}
(d_0^n + S)\|\vec{\Psi}^{n+1}\|_\infty &\leq \|((d_0^n + S)I - \varepsilon^2 \Lambda^{*,n+1} D_h) \vec{\Psi}^{n+1}\|_\infty \\
&\leq \sum_{k=0}^n \|Q_{n-k}^n\|_\infty \|\vec{\Psi}^k\|_\infty + \|S\vec{\Phi}^{*,n+1} - f(\vec{\Phi}^{*,n+1})\|_\infty \\
&\leq (1 - \eta_*) \sum_{k=1}^n (d_{n-k}^n - d_{n+1-k}^n - S\eta_*^{n+1-k}) + (d_n^n - d_{n+1}^n - S\eta_*^{n+1}) + S \\
&= (d_0^n + S)(1 - \eta_*).
\end{aligned}$$

which gives  $\|\vec{\Psi}^{n+1}\|_\infty \leq 1 - \eta_*$ . The proof is completed.  $\square$

#### 4. ERROR ANALYSIS AND ENERGY STABILITY

In this section, we investigate the error estimate and energy stability of the proposed BDF2 scheme (2.15). Let  $\Phi(t) = \Pi_{C_h} \phi(t)$  where  $\phi$  denotes the exact solution of (1.1). We also use  $C$  and  $C_i$ 's to denote some needed generic positive constants independent of  $h$  and  $\tau$ .

##### 4.1. Discrete $H^1$ error estimate and energy stability for the constant mobility case.

In this subsection, we study the discrete  $H^1$  error estimate and energy stability of the BDF2 scheme (2.15) for the Allen-Cahn equation with constant mobility, i.e.,  $M(\phi) \equiv C > 0$ . Without loss of generality, we assume  $M(\phi) \equiv 1$  and thus (2.13) becomes  $S \geq 2$ . Firstly, we recall a useful



Taking the discrete  $L^2$  inner products of (4.4a) and (4.4b) with  $2\tau_{n+1}e^{*,n+1}$  and  $2(e^{n+1} - e^n)$ , respectively, we obtain by Lemma 2.1 that

$$\begin{aligned} & \|e^{*,n+1}\|_h^2 - \|e^n\|_h^2 + 2\tau_{n+1}\varepsilon^2\|\nabla_h e^{*,n+1}\|_h^2 + 2\tau_{n+1}S\|e^{*,n+1}\|_h^2, \\ & = 2\tau_{n+1}\langle Se^n - S(\vec{\Phi}(t_{n+1}) - \vec{\Phi}(t_n)) + f(\vec{\Phi}(t_{n+1})) - f(\vec{\Phi}^n) + T_1^n + T_2^n, e^{*,n+1}\rangle_\Omega, \end{aligned} \quad (4.5a)$$

$$\begin{aligned} & 2\langle F_2^{n+1}e, e^{n+1} - e^n \rangle_\Omega + \varepsilon^2(\|\nabla_h e^{n+1}\|_h^2 - \|\nabla_h e^n\|_h^2) + S(\|e^{n+1}\|_h^2 - \|e^n\|_h^2) \\ & \leq 2\langle Se^{*,n+1} + f(\vec{\Phi}(t_{n+1})) - f(\vec{\Phi}^{*,n+1}) + T_2^n + T_3^n, e^{n+1} - e^n \rangle_\Omega. \end{aligned} \quad (4.5b)$$

For (4.5b), using the inequality (4.1), Cauchy-Schwarz inequality and Young's inequality, we have

$$\begin{aligned} & \frac{\gamma_{n+2}^{3/2}}{1 + \gamma_{n+2}} \frac{\|e^{n+1} - e^n\|_h^2}{\tau_{n+1}} - \frac{\gamma_{n+1}^{3/2}}{1 + \gamma_{n+1}} \frac{\|e^n - e^{n-1}\|_h^2}{\tau_n} + G(\gamma_*, \gamma_*) \frac{\|e^{n+1} - e^n\|_h^2}{\tau_{n+1}} \\ & + \varepsilon^2(\|\nabla_h e^{n+1}\|_h^2 - \|\nabla_h e^n\|_h^2) + S(\|e^{n+1}\|_h^2 - \|e^n\|_h^2) \\ & \leq C_3\tau_{n+1}(\|e^{*,n+1}\|_h^2 + \|f(\vec{\Phi}(t_{n+1})) - f(\vec{\Phi}^{*,n+1})\|_h^2 + \|T_2^n\|_h^2 + \|T_3^n\|_h^2) \\ & \quad + G(\gamma_*, \gamma_*) \frac{\|e^{n+1} - e^n\|_h^2}{\tau_{n+1}} \\ & \leq C_3 \max\{1, (C_2)^2\} \tau_{n+1} (\|e^{*,n+1}\|_h^2 + \|T_2^n\|_h^2 + \|T_3^n\|_h^2) + G(\gamma_*, \gamma_*) \frac{\|e^{n+1} - e^n\|_h^2}{\tau_{n+1}}, \end{aligned} \quad (4.6)$$

where we have used the fact

$$\|f(\vec{\Phi}(t_{n+1})) - f(\vec{\Phi}^{*,n+1})\|_h^2 \leq (C_2)^2 \|e^{*,n+1}\|_h^2$$

derived from (4.3). Thus we deduce that

$$\begin{aligned} & \frac{\gamma_{n+2}^{3/2}}{1 + \gamma_{n+2}} \frac{\|e^{n+1} - e^n\|_h^2}{\tau_{n+1}} - \frac{\gamma_{n+1}^{3/2}}{1 + \gamma_{n+1}} \frac{\|e^n - e^{n-1}\|_h^2}{\tau_n} + \varepsilon^2(\|\nabla_h e^{n+1}\|_h^2 - \|\nabla_h e^n\|_h^2) \\ & + S(\|e^{n+1}\|_h^2 - \|e^n\|_h^2) \leq C_3 \max\{1, (C_2)^2\} \tau_{n+1} (\|e^{*,n+1}\|_h^2 + \|T_2^n\|_h^2 + \|T_3^n\|_h^2). \end{aligned} \quad (4.7)$$

In a similar way, we can obtain the following estimate from (4.5a)

$$\begin{aligned} & \|e^{*,n+1}\|_h^2 - \|e^n\|_h^2 + 2\tau_{n+1}\varepsilon^2\|\nabla_h e^{*,n+1}\|_h^2 + 2\tau_{n+1}S\|e^{*,n+1}\|_h^2 \\ & \leq C_4\tau_{n+1}^2(\|e^n\|_h^2 + \|\vec{\Phi}(t_{n+1}) - \vec{\Phi}(t_n)\|_h^2 + \|f(\vec{\Phi}(t_{n+1})) - f(\vec{\Phi}^n)\|_h^2 \\ & \quad + \|T_1^n\|_h^2 + \|T_2^n\|_h^2) + \frac{1}{2}\|e^{*,n+1}\|_h^2 \\ & \leq C_5\tau_{n+1}^2(\|e^n\|_h^2 + \tau_{n+1}^2\|\phi_t\|_{L^\infty(0,T;L^\infty(\Omega))}^2 + \|T_1^n\|_h^2 + \|T_2^n\|_h^2) + \frac{1}{2}\|e^{*,n+1}\|_h^2, \end{aligned} \quad (4.8)$$

where we have used the fact

$$\begin{aligned} \|f(\vec{\Phi}(t_{n+1})) - f(\vec{\Phi}^n)\|_h^2 & \leq \|f(\vec{\Phi}(t_{n+1})) - f(\vec{\Phi}(t_n))\|_h^2 + \|f(\vec{\Phi}(t_n)) - f(\vec{\Phi}^n)\|_h^2 \\ & \leq (C_2)^2(\|\vec{\Phi}(t_{n+1}) - \vec{\Phi}(t_n)\|_h^2 + \|e^n\|_h^2) \\ & \leq (C_2)^2(\tau_{n+1}^2\|\phi_t\|_{L^\infty(0,T;L^\infty(\Omega))}^2 + \|e^n\|_h^2). \end{aligned}$$

Then it follows from (4.8) that

$$\|e^{*,n+1}\|_h^2 \leq 2\|e^n\|_h^2 + 2C_5\tau_{n+1}^2(\|e^n\|_h^2 + \tau_{n+1}^2\|\phi_t\|_{L^\infty(0,T;L^\infty(\Omega))}^2 + \|T_1^n\|_h^2 + \|T_2^n\|_h^2). \quad (4.9)$$

Combining with (4.7) and (4.9), gives

$$\begin{aligned} & \frac{\gamma_{n+2}^{3/2}}{1 + \gamma_{n+2}} \frac{\|e^{n+1} - e^n\|_h^2}{\tau_{n+1}} - \frac{\gamma_{n+1}^{3/2}}{1 + \gamma_{n+1}} \frac{\|e^n - e^{n-1}\|_h^2}{\tau_n} + \varepsilon^2 (\|\nabla_h e^{n+1}\|_h^2 - \|\nabla_h e^n\|_h^2) \\ & + S(\|e^{n+1}\|_h^2 - \|e^n\|_h^2) \\ & \leq C_6 \tau_{n+1} (\|e^n\|_h^2 + \tau_{n+1}^4 \|\phi_t\|_{L^\infty(0,T;L^\infty(\Omega))}^2) + \tau_{n+1}^2 \|T_1^n\|_h^2 + \|T_2^n\|_h^2 + \|T_3^n\|_h^2. \end{aligned} \quad (4.10)$$

For the truncation errors  $T_i^n$ ,  $i = 1, 2, 3$ , we have the following estimates (see [38, 41]):

$$\begin{aligned} \|T_1^n\|_h^2 & \leq C_7 \tau_{n+1}^2 \|\phi\|_{W^{2,\infty}(0,T;L^\infty(\Omega))}^2, \quad \|T_2^n\|_h^2 \leq C_8 h^4 \|\phi\|_{L^\infty(0,T;W^{4,\infty}(\Omega))}^2, \\ \|T_3^n\|_h^2 & \leq C_9 (\tau_n + \tau_{n+1})^4 \|\phi\|_{W^{3,\infty}(0,T;L^\infty(\Omega))}^2. \end{aligned} \quad (4.11)$$

Thus, summing up the inequality (4.10) from 1 to  $n$  gives

$$\begin{aligned} & \frac{\gamma_{n+2}^{3/2}}{1 + \gamma_{n+2}} \frac{\|e^{n+1} - e^n\|_h^2}{\tau_{n+1}} + \varepsilon^2 \|\nabla_h e^{n+1}\|_h^2 + S \|e^{n+1}\|_h^2 \\ & \leq \frac{\gamma_2^{3/2}}{1 + \gamma_2} \frac{\|e^1\|_h^2}{\tau_1} + \varepsilon^2 \|\nabla_h e^1\|_h^2 + S \|e^1\|_h^2 + C_{10} \sum_{k=1}^n \tau_{k+1} \|e^k\|_h^2 \\ & \quad + C_{11} (\tau^4 \|\phi\|_{W^{3,\infty}(0,T;L^\infty(\Omega))}^2 + h^4 \|\phi\|_{L^\infty(0,T;W^{4,\infty}(\Omega))}^2). \end{aligned} \quad (4.12)$$

For the case of  $n = 0$ , the corresponding error equation (by BDF1) reads as

$$\frac{e^1}{\tau_1} - \varepsilon^2 \Delta_h e^1 + S e^1 = f(\vec{\Phi}(t_1)) - f(\vec{\Phi}^0) + T_2^0 + T_3^0.$$

Similar to the arguments for the case  $n \geq 1$ , the following estimate can be derived under the assumption  $\tau_1 \leq C_1 \tau^{4/3}$ :

$$\frac{\|e^1\|_h^2}{\tau_1} + \varepsilon^2 \|\nabla_h e^1\|_h^2 + S \|e^1\|_h^2 \leq C_{12} \tau_1 (\tau_1^2 + h^4) \leq C_{12} \max\{1, (C_1)^3\} (\tau^4 + h^4). \quad (4.13)$$

Combining (4.12) and (4.13) and using the discrete Gronwall's lemma, we then obtain the desired estimate (4.2).  $\square$

**Remark 4.1.** *It often imposes a further restriction on the time step size when using the Gronwall's inequality for the error analysis. However, in the above proof of Theorem 4.1, we note that the term  $G(\gamma_*, \gamma_*) \frac{\|e^{n+1} - e^n\|_h^2}{\tau_{n+1}}$  on the right-hand side of the error inequality (4.6) can be eliminated by a term from the left-hand side of the equation. Consequently, we are able to obtain the error inequality (4.12), which only contains the norm terms of  $e^{n+1}$  with positive coefficients on the left-hand side. Thus, there is no further time step restriction from the use of the Gronwall's inequality in our error analysis.*

With the help of the MBP property (Theorem 3.1) and the discrete  $H^1$  error estimate (Theorem 4.1), we are able to achieve the energy stability property of the BDF2 scheme (2.15).

**Theorem 4.2.** *Under the assumption of Theorem 4.1, the BDF2 scheme (2.15) in the constant mobility case is energy stable in the sense that*

$$E_h^{n+1} - E_h^n \leq C(h^4 + \tau^2) \quad (4.14)$$

for all  $0 \leq n \leq N-1$ , where the modified discrete energy  $E_h^n$  is defined by

$$E_h^n = E_h(\vec{\Phi}^n) + \frac{\gamma_{n+1}^{3/2} \|\vec{\Phi}^n - \vec{\Phi}^{n-1}\|_h^2}{1 + \gamma_{n+1} \quad 2\tau_n}.$$

*Proof.* Taking the discrete  $L^2$ -inner product of (2.15) with  $\vec{\Phi}^{n+1} - \vec{\Phi}^n$ , we get that

$$\begin{aligned} & \langle F_2^{n+1} \vec{\Phi}, \vec{\Phi}^{n+1} - \vec{\Phi}^n \rangle_\Omega + \varepsilon^2 \langle \nabla_h \vec{\Phi}^{n+1}, \nabla_h (\vec{\Phi}^{n+1} - \vec{\Phi}^n) \rangle_\Omega + \langle f(\vec{\Phi}^{n+1}), \vec{\Phi}^{n+1} - \vec{\Phi}^n \rangle_\Omega \\ &= \langle f(\vec{\Phi}^{n+1}) - f(\vec{\Phi}^{*,n+1}), \vec{\Phi}^{n+1} - \vec{\Phi}^n \rangle_\Omega - S \langle \vec{\Phi}^{n+1} - \vec{\Phi}^{*,n+1}, \vec{\Phi}^{n+1} - \vec{\Phi}^n \rangle_\Omega \\ &\leq \frac{(C_2)^2 + S^2}{2} \|\vec{\Phi}^{n+1} - \vec{\Phi}^{*,n+1}\|_h^2 + \|\vec{\Phi}^{n+1} - \vec{\Phi}^n\|_h^2 \\ &\leq \max \left\{ \frac{1}{2} ((C_2)^2 + S^2), 1, \|\phi_t\|_{L^\infty(0,T;L^\infty(\Omega))} \right\} (\|e^n\|_h^2 + \|e^{n+1}\|_h^2 + \|e^{*,n+1}\|_h^2 + \tau_{n+1}^2), \end{aligned} \quad (4.15)$$

where we have used the following inequalities

$$\begin{aligned} \|\vec{\Phi}^{n+1} - \vec{\Phi}^{*,n+1}\|_h^2 &= \|\vec{\Phi}^{n+1} - \vec{\Phi}(t_{n+1}) + \vec{\Phi}(t_{n+1}) - \vec{\Phi}^{*,n+1}\|_h^2 \\ &\leq \|e^{n+1}\|_h^2 + \|e^{*,n+1}\|_h^2, \\ \|\vec{\Phi}^{n+1} - \vec{\Phi}^n\|_h^2 &= \|\vec{\Phi}^{n+1} - \vec{\Phi}(t_{n+1}) + \vec{\Phi}(t_{n+1}) - \vec{\Phi}(t_n) + \vec{\Phi}(t_n) - \vec{\Phi}^n\|_h^2 \\ &\leq \|e^{n+1}\|_h^2 + \tau_{n+1}^2 \|\phi_t\|_{L^\infty(0,T;L^\infty(\Omega))} + \|e^n\|_h^2. \end{aligned}$$

Noting that

$$\begin{aligned} a(a-b) &= \frac{1}{2}(a^2 - b^2 + (a-b)^2), \quad a, b \in \mathbb{R}, \\ \langle F(\vec{\Phi}^{n+1}) - F(\vec{\Phi}^n), 1 \rangle_\Omega &\leq \langle f(\vec{\Phi}^{n+1}), \vec{\Phi}^{n+1} - \vec{\Phi}^n \rangle_\Omega + \frac{1}{2} \|\vec{\Phi}^{n+1} - \vec{\Phi}^n\|_h^2, \end{aligned}$$

and using (4.1) and (4.15), we can derive

$$\begin{aligned} E_h^{n+1} - E_h^n &\leq \max \left\{ \frac{1}{2} ((C_2)^2 + S^2), \frac{3}{2}, \frac{3}{2} \|\phi_t\|_{L^\infty(0,T;L^\infty(\Omega))} \right\} \\ &\quad \cdot (\|e^n\|_h^2 + \|e^{n+1}\|_h^2 + \|e^{*,n+1}\|_h^2 + \tau_{n+1}^2). \end{aligned} \quad (4.16)$$

Combining with (4.2), (4.9), and (4.16), we then obtain (4.14).  $\square$

**Remark 4.2.** For the quasi-uniform temporal mesh, there exists a finite constant  $\beta$  such that  $\max_{1 \leq n \leq N} \tau_n / \min_{1 \leq n \leq N} \tau_n \leq \beta$  and thus  $\tau \leq \frac{\beta T}{N}$ . When  $\tau$  is sufficient small and  $h = O(\sqrt{\tau})$ , we can obtain

$$E_h(\vec{\Phi}^n) \leq E_h^n \leq E_h^1 + C \leq E_h(\vec{\Phi}^0) + C, \quad \forall 1 \leq n \leq N$$

for the BDF2 scheme (2.15) in the constant mobility case.

**Remark 4.3.** The inequality (4.1) plays an important role in the above error and energy stability analysis. Unfortunately, we have not been able to prove a similar result as (4.1) for the estimate of  $\langle (\Lambda^{*,n+1})^{-1} F_2^{n+1} \vec{\Phi}, \vec{\Phi}^{n+1} - \vec{\Phi}^n \rangle_\Omega$  in the case of variable mobility. Thus the results in Theorems 4.1 and 4.2 could not be applied to the variable mobility case, and deeper analysis for this issue certainly needs more efforts.

**4.2. Error estimate in the  $L^\infty$  norm for the general mobility case.** In this subsection, we study the discrete  $L^\infty$  error estimate of the BDF2 scheme (2.15) for the Allen-Cahn equation with a general mobility  $M(\phi)$ . Let us define

$$F_2 \vec{\Phi}(t_{n+1}) = b_0^n (\vec{\Phi}(t_{n+1}) - \vec{\Phi}(t_n)) + b_1^n (\vec{\Phi}(t_n) - \vec{\Phi}(t_{n-1}))$$

for  $1 \leq n \leq N-1$  and  $\Lambda(\vec{\Phi}(t_n)) = \text{diag}(M(\vec{\Phi}(t_n)))$  for  $0 \leq n \leq N-1$ .

**Lemma 4.1.** *Assume that  $\{g^k\}_{k=0}^{N-1}$  and  $\{\omega^k\}_{k=0}^N$  are two non-negative sequences and there exist some constants  $\zeta > 0$  and  $\lambda \in (0, 1)$  such that*

$$\sum_{k=1}^{n+1} d_{n-k+1}^n \delta_\tau \omega^k \leq \zeta \sum_{k=0}^n \lambda^{n-k} \omega^k + g^n, \quad \forall 0 \leq n \leq N-1, \quad (4.17)$$

where the discrete kernels  $\{d_k^n\}_{k=0}^n$  are defined in (2.4). Then it holds

$$\omega^{n+1} \leq \exp\left(\frac{\zeta t_{n+1}}{1-\lambda}\right) \left(\omega^0 + \sum_{k=0}^n \frac{g^k}{b_0^k}\right). \quad (4.18)$$

The proof of this lemma is similar to that of Lemma 5.1 in [41] and Theorem 3.1 in [40] by using the technique of the discrete complementary convolution kernels of  $\{d_k^n\}_{k=0}^n$ . We omit it here and leave it for the interested readers. Comparing with Lemma 5.1 in [41] and Theorem 3.1 in [40], there is no term  $\omega^{n+1}$  on the right-hand side of the condition (4.17). Then the time step restriction required in [41] and [40] for the result (4.18) can be removed.

**Theorem 4.3.** *Assume that  $0 < \gamma_n \leq \gamma_* < 1 + \sqrt{2}$  for all  $1 \leq n \leq N-1$ ,  $M(\cdot) \in C^1(\mathbb{R})$ , the stabilizing parameter satisfies (2.13), and the time step sizes satisfy (3.8) and (3.11). Let  $\gamma_{N+1}$  be any number in  $(0, \gamma_*)$ . In addition, assume  $\phi \in W^{3,\infty}(0, T; L^\infty(\Omega)) \cap L^\infty(0, T; W^{4,\infty}(\Omega))$ . Then it holds for the BDF2 scheme (2.15) in the general mobility case that*

$$\|e^{n+1}\|_\infty \leq \frac{C_1 t_{n+1}}{1-\eta_*} \exp\left(\frac{C_2 t_{n+1}}{1-\eta_*}\right) (\tau^2 \|\phi\|_{W^{3,\infty}(0,T;L^\infty(\Omega))} + h^2 \|\phi\|_{L^\infty(0,T;W^{4,\infty}(\Omega))}) \quad (4.19)$$

for all  $0 \leq n \leq N-1$ .

*Proof.* From (1.1), we deduce that the exact solution  $\vec{\Phi}$  satisfies the following equation: for any  $1 \leq n \leq N-1$ ,

$$F_2 \vec{\Phi}(t_{n+1}) + \Lambda(\vec{\Phi}(t_{n+1})) (-\varepsilon^2 D_h \vec{\Phi}(t_{n+1}) + F'(\vec{\Phi}(t_{n+1}))) + \mathcal{T}_2^n + \mathcal{T}_3^n = 0, \quad (4.20)$$

where

$$\mathcal{T}_2^n = \Lambda(\vec{\Phi}(t_{n+1})) (-\varepsilon^2 \Delta \vec{\Phi}(t_{n+1}) + \varepsilon^2 D_h \vec{\Phi}(t_{n+1})), \quad \mathcal{T}_3^n = \vec{\Phi}_t(t_{n+1}) - \partial_t(\Pi_{2,n} \vec{\Phi})(t_{n+1}).$$

It is easy to verify that

$$\|\mathcal{T}_2^n\|_\infty \leq C_3 h^2 \|\phi\|_{L^\infty(0,T;W^{4,\infty}(\Omega))}, \quad \|\mathcal{T}_3^n\|_\infty \leq C_4 (\tau_n + \tau_{n+1})^2 \|\phi\|_{W^{3,\infty}(0,T;L^\infty(\Omega))}.$$

Subtracting (2.16b) from (4.20), we derive the error equation of  $e^{n+1}$  as

$$\begin{aligned} & F_2^{n+1} e + S e^{n+1} - \varepsilon^2 \Lambda^{*,n+1} D_h e^{n+1} \\ &= S e^{*,n+1} - \Lambda^{*,n+1} (F'(\vec{\Phi}^{*,n+1}) - F'(\vec{\Phi}(t_{n+1}))) - (\Lambda^{*,n+1} - \Lambda(\vec{\Phi}(t_{n+1}))) \\ & \quad (-\varepsilon^2 D_h \vec{\Phi}(t_{n+1}) + F'(\vec{\Phi}(t_{n+1}))) + \mathcal{T}_2^n + \mathcal{T}_3^n =: I^n. \end{aligned} \quad (4.21)$$



Since  $F(\rho) = (1 - \rho^2)^2/4$ , we have  $\max_{\rho \in [-1,1]} F'(\rho) = \frac{2}{3\sqrt{3}}$  and  $\max_{\rho \in [-1,1]} F''(\rho) = 2$ . Therefore, we can get

$$\|\Lambda^{*,n+1} - \Lambda(\vec{\Phi}(t_{n+1}))\|_\infty \leq \max_{\rho \in [-1,1]} |M'(\rho)| \|e^{*,n+1}\|_\infty,$$

and thus

$$\begin{aligned} \|I^n\|_\infty &\leq S \|e^{*,n+1}\|_\infty + 2L \|e^{*,n+1}\|_\infty + \left( \varepsilon^2 \|\phi\|_{L^\infty(0,T;W^{2,\infty}(\Omega))} + \frac{2}{3\sqrt{3}} \right) \\ &\quad \|\Lambda^{*,n+1} - \Lambda(\vec{\Phi}(t_{n+1}))\|_\infty + \|\mathcal{T}_2^n\|_\infty + \|\mathcal{T}_3^n\|_\infty \\ &\leq C_4 \|e^{*,n+1}\|_\infty + C_5 [\tau^2 \|\phi\|_{W^{3,\infty}(0,T;L^\infty(\Omega))} + h^2 \|\phi\|_{L^\infty(0,T;W^{4,\infty}(\Omega))}], \end{aligned} \quad (4.22)$$

where  $L$  is defined in Lemma 3.1,

$$C_4 = S + 2L + \max_{\rho \in [-1,1]} |M'(\rho)| \left( \varepsilon^2 \|\phi\|_{L^\infty(0,T;W^{2,\infty}(\Omega))} + \frac{2}{3\sqrt{3}} \right) = S + 2L + C_6, \quad (4.23)$$

and we have used the fact

$$\|\varepsilon^2 D_h \vec{\Phi}(t_{n+1})\|_\infty = \|\varepsilon^2 \Delta \vec{\Phi}(t_{n+1}) + \mathcal{T}_2^n\|_\infty \leq \varepsilon^2 \|\phi\|_{L^\infty(0,T;W^{2,\infty}(\Omega))} + \|\mathcal{T}_2^n\|_\infty. \quad (4.24)$$

Following the similar process of deriving (4.21), we can easily obtain the error equation of  $e^{*,n+1}$  from (1.1) and (2.16a) as:

$$\begin{aligned} \frac{e^{*,n+1} - e^n}{\tau_{n+1}} + S e^{*,n+1} - \varepsilon^2 \Lambda^n D_h e^{*,n+1} \\ = S e^n - S(\vec{\Phi}(t_{n+1}) - \vec{\Phi}(t_n)) - \Lambda^n [F'(\vec{\Phi}^n) - F'(\vec{\Phi}(t_{n+1}))] \\ - [\Lambda^n - \Lambda(\vec{\Phi}(t_{n+1}))] [-\varepsilon^2 D_h \vec{\Phi}(t_{n+1}) + F'(\vec{\Phi}(t_{n+1}))] + \mathcal{T}_1^n + \mathcal{T}_2^n, \end{aligned} \quad (4.25)$$

where  $\mathcal{T}_1^n = \vec{\Phi}(t_{n+1}) - \frac{\vec{\Phi}(t_{n+1}) - \vec{\Phi}(t_n)}{\tau_{n+1}}$  satisfies

$$\|\mathcal{T}_1^n\|_\infty \leq C_7 \tau_{n+1} \|\phi\|_{W^{2,\infty}(0,T;L^\infty(\Omega))}.$$

Noting that

$$\begin{aligned} \|F'(\vec{\Phi}^n) - F'(\vec{\Phi}(t_{n+1}))\|_\infty &= \|F'(\vec{\Phi}^n) + F'(\vec{\Phi}(t_n))\|_\infty + \|F'(\vec{\Phi}(t_n)) - F'(\vec{\Phi}(t_{n+1}))\|_\infty \\ &\leq 2[\|e^n\|_\infty + \|\phi\|_{W^{1,\infty}(0,T;L^\infty(\Omega))} \tau_{n+1}], \\ \|\Lambda^n - \Lambda(\vec{\Phi}(t_{n+1}))\|_\infty &\leq \|\Lambda^n - \Lambda(\vec{\Phi}(t_n))\|_\infty + \|\Lambda(\vec{\Phi}(t_n)) - \Lambda(\vec{\Phi}(t_{n+1}))\|_\infty \\ &\leq \max_{\rho \in [-1,1]} |M'(\rho)| [\|e^n\|_\infty + \tau_{n+1} \|\phi\|_{W^{1,\infty}(0,T;L^\infty(\Omega))}]. \end{aligned}$$

Multiplying (4.25) with  $\tau_{n+1}$ , and combining it with (4.23) and (4.24), we derive that

$$\begin{aligned} (1 + S\tau_{n+1}) \|e^{*,n+1}\|_\infty &\leq \|e^{*,n+1} + S\tau_{n+1} e^{*,n+1} - \varepsilon^2 \tau_{n+1} \Lambda^n D_h e^{*,n+1}\|_\infty \\ &\leq (1 + \tau_{n+1}(S + 2L + C_6)) \|e^n\|_\infty \\ &\quad + C_8 (\tau_{n+1}^2 \|\phi\|_{W^{2,\infty}(0,T;L^\infty(\Omega))} + \tau_{n+1} h^2 \|\phi\|_{L^\infty(0,T;W^{4,\infty}(\Omega))}). \end{aligned}$$

Therefore, we obtain

$$\|e^{*,n+1}\|_\infty \leq C_9 \|e^n\|_\infty + C_{10} (\tau_{n+1}^2 \|\phi\|_{W^{2,\infty}(0,T;L^\infty(\Omega))} + \tau_{n+1} h^2 \|\phi\|_{L^\infty(0,T;W^{4,\infty}(\Omega))}), \quad (4.26)$$

where  $C_9 = 1 + (2L + C_6)\tau_{n+1} \geq \frac{1 + \tau_{n+1}(S + 2L + C_6)}{1 + S\tau_{n+1}}$ .

Define  $\bar{e}^{n+1} = e^{n+1} - \eta_* e^n$  for  $0 \leq n \leq N-1$  with  $\bar{e}^0 = e^0 = 0$ . Then we have

$$\bar{e}^1 = e^1, \quad e^{n+1} = \sum_{k=0}^{n+1} \eta_*^{n+1-k} \bar{e}^k, \quad 1 \leq n \leq N-1, \quad (4.27)$$

and it is easy to check that

$$\|\bar{e}^1\|_\infty = \|e^1\|_\infty \leq C_{11}(\tau_1^2 \|\phi\|_{W^{2,\infty}(0,T;L^\infty(\Omega))} + \tau_1 h^2 \|\phi\|_{L^\infty(0,T;W^{4,\infty}(\Omega))})$$

with the BDF1 scheme as the starting step. Using the similar process to derive (3.2) from (2.16b), we can obtain the following equation for  $\bar{e}^{n+1}$  from (4.21):

$$((d_0^n + S)I - \varepsilon^2 \Lambda^{*,n+1} D_h) \bar{e}^{n+1} = \sum_{k=0}^n Q_{n-k}^n \bar{e}^k + I^n, \quad (4.28)$$

where  $Q_k^n$  is defined in (3.3) with  $\eta = \eta_*$ . Consequently, we can use Lemma 3.2 and (4.28) to get

$$\begin{aligned} d_0^n \|\bar{e}^{n+1}\|_\infty &\leq \|((d_0^n + S)I - \varepsilon^2 \Lambda^{*,n+1} D_h) \bar{e}^{n+1}\|_\infty \\ &\leq \sum_{k=0}^n (d_{n-k}^n - d_{n-k+1}^n - S \eta_*^{n+1-k}) \|\bar{e}^k\|_\infty + \|I^n\|_\infty \\ &\leq \sum_{k=0}^n (d_{n-k}^n - d_{n-k+1}^n) \|\bar{e}^k\|_\infty + \|I^n\|_\infty. \end{aligned}$$

Rewriting the above inequality gives  $\sum_{k=1}^{n+1} d_{n-k+1}^n \delta_\tau \|\bar{e}^k\|_\infty \leq \|I^n\|_\infty$ . Combining it with (4.22), (4.26) and (4.27), we obtain

$$\begin{aligned} \sum_{k=1}^{n+1} d_{n-k+1}^n \delta_\tau \|\bar{e}^k\|_\infty &\leq C_2 \|e^k\|_\infty + C_{12}(\tau^2 \|\phi\|_{W^{3,\infty}(0,T;L^\infty(\Omega))} + h^2 \|\phi\|_{L^\infty(0,T;W^{4,\infty}(\Omega))}) \\ &\leq C_2 \sum_{k=1}^n \eta_*^{n-k} \|\bar{e}^k\|_\infty + C_{12}(\tau^2 \|\phi\|_{W^{3,\infty}(0,T;L^\infty(\Omega))} \\ &\quad + h^2 \|\phi\|_{L^\infty(0,T;W^{4,\infty}(\Omega))}) \end{aligned} \quad (4.29)$$

with  $C_2 = C_4 C_8$ . Next, it follows from Lemma 4.1 that

$$\begin{aligned} \|\bar{e}^{n+1}\|_\infty &\leq C_1 \exp\left(\frac{C_2 t_{n+1}}{1 - \eta_*}\right) (\tau^2 \|\phi\|_{W^{3,\infty}(0,T;L^\infty(\Omega))} + h^2 \|\phi\|_{L^\infty(0,T;W^{4,\infty}(\Omega))}) \sum_{k=0}^n \frac{1}{b_0^k} \\ &\leq C_1 t_{n+1} \exp\left(\frac{C_2 t_{n+1}}{1 - \eta_*}\right) (\tau^2 \|\phi\|_{W^{3,\infty}(0,T;L^\infty(\Omega))} + h^2 \|\phi\|_{L^\infty(0,T;W^{4,\infty}(\Omega))}), \end{aligned}$$

where we have used the fact that  $\frac{1}{b_0^0} = \tau_1$  and  $\frac{1}{b_0^k} = \frac{1 + \gamma_{k+1}}{1 + 2\gamma_{k+1}} \tau_{k+1} \leq \tau_{k+1}$  for  $1 \leq k \leq n$ . Finally, we obtain

$$\begin{aligned} \|e^{n+1}\|_\infty &\leq \sum_{k=1}^{n+1} \eta_*^{n+1-k} \|\bar{e}^k\|_\infty \\ &\leq \frac{C_1 t_{n+1}}{1 - \eta_*} \exp\left(\frac{C_2 t_{n+1}}{1 - \eta_*}\right) (\tau^2 \|\phi\|_{W^{3,\infty}(0,T;L^\infty(\Omega))} + h^2 \|\phi\|_{L^\infty(0,T;W^{4,\infty}(\Omega))}), \end{aligned}$$

which completes the proof.  $\square$

**Remark 4.4.** *Similar to the derivation of linear BDF2 scheme (2.15), one can also construct a linear second order in time scheme with variable time step sizes based on the Crank-Nicolson formulation as follows: given  $\Phi^0 = \Pi_{C_h} \phi_0$ , and for  $n = 1, 2 \dots, N-1$ , find  $\Phi^{n+1} \in C_h$  such that*

$$\begin{cases} \Phi^{n+\frac{1}{2}} = \text{BDF1}(\Phi^n, \tau_{n+1}/2), & (4.30a) \\ \frac{\Phi^{n+1} - \Phi^n}{\tau_{n+1}} - \varepsilon^2 M(\Phi^{n+\frac{1}{2}}) \Delta_h \frac{\Phi^{n+1} + \Phi^n}{2} + f(\Phi^{n+\frac{1}{2}}) + S\left(\frac{\Phi^{n+1} + \Phi^n}{2} - \Phi^{n+\frac{1}{2}}\right) = 0, & (4.30b) \end{cases}$$

The above theoretical analysis for the BDF2 scheme (2.15) can be applied to the Crank-Nicolson scheme (4.30) to derive similar results obtained for the BDF2 scheme (2.15), including the conditional MBP preserving and corresponding error estimates.

## 5. NUMERICAL RESULTS

In this section we perform various experiments on the Allen-Cahn equation (1.1) to numerically validate the theoretical results of the proposed BDF2 scheme (2.15) in terms of accuracy and preservation of the MBP. The homogenous Neumann boundary condition is always imposed.

**5.1. Test of temporal convergence.** We consider two types of mobility functions: one is the constant mobility  $M(\phi) \equiv 1$  and the other is the nonlinear degenerate mobility  $M(\phi) = 1 - \phi^2$ . We choose  $\Omega = (0, 1)^2$ ,  $\varepsilon = 0.1$ , the initial value

$$\phi_0(x, y) = 0.1(\cos 3x \cos 2y + \cos 5x \cos 5y),$$

and the terminal time  $T = 1$ . The stabilizing parameter is set to be  $S = 2$  to satisfy the requirement (2.13) for both mobility functions.

The central finite difference method is used for the spatial discretization with the fixed small mesh size  $h = 1/1024$ . Since there is no analytical solution available for this example to exactly evaluate the numerical solution errors, we instead compute their approximations in the discrete  $L^\infty$  and  $H^1$  norms, respectively:

$$e_\infty^T = \|\vec{\Phi}^N - \vec{\Phi}^{2N}\|_\infty, \quad e_{H^1}^T = \|\vec{\Phi}^N - \vec{\Phi}^{2N}\|_{H_h^1},$$

where  $\vec{\Phi}^N$  and  $\vec{\Phi}^{2N}$  denote the numerical solution at the terminal time  $T = 1$  with  $N$  and  $2N$  subintervals for the time domain  $[0, 1]$ , respectively. To validate the theoretical temporal accuracy, we firstly investigate the error behaviors of the BDF2 scheme (2.15) with the uniform time steps by repeatedly refining the time step size  $\tau$  from  $1/10$  to  $1/640$  (i.e.,  $N$  changes from 10 to 640). The solution errors vs. the time step sizes are plotted in Fig. 1 in the log-log scale for both mobility functions. It is observed that the BDF2 scheme (2.15) achieves the expected second-order temporal accuracy for all test cases. Next, we numerically study the error behaviors of the BDF2 scheme (2.15) with nonuniform time steps. The nonuniform time step sizes  $\{\widehat{t}_n\}_{n=0}^N$  used here is produced by 25% perturbation of the uniform ones  $\{t_n = n/N\}_{n=0}^N$ . As reported in Table 1, the second-order temporal accuracy is still achieved by the BDF2 scheme for all cases.

**5.2. Test of MBP preservation.** We demonstrate the MBP preservation of the proposed BDF2 scheme (2.15) through two well-known benchmark examples governed by the Allen-Cahn equations. One is the shrinking bubble problem [5] and the other is the grain coarsening problem.

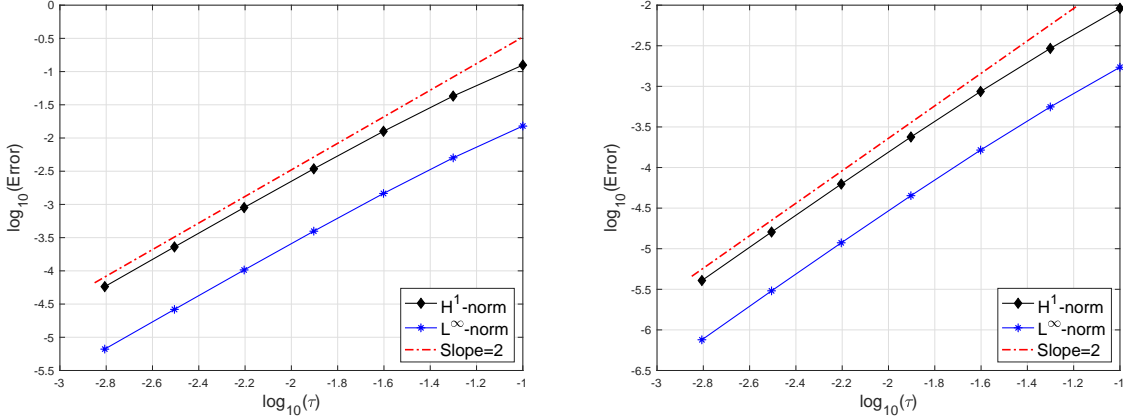


FIGURE 1. Plots of the numerical solution errors vs. the time step sizes in the log-log scale for the BDF2 scheme (2.15) with uniform time steps. Left:  $M(\phi) \equiv 1$ ; right:  $M(\phi) = 1 - \phi^2$ .

TABLE 1. Numerical solution errors and convergence rates of the BDF2 scheme (2.15) with nonuniform time steps.

Time steps			$M(\phi) \equiv 1$				$M(\phi) = 1 - \phi^2$			
$N$	$\tau$	$\max\{\gamma_n\}$	$e_\infty^T$	Order	$e_{H^1_h}^T$	Order	$e_\infty^T$	Order	$e_{H^1_h}^T$	Order
10	1.393e-1	2.282	1.669e-2	—	1.375e-1	—	1.886e-3	—	1.005e-2	—
20	7.033e-2	2.358	5.834e-3	1.54	4.941e-2	1.50	6.399e-4	1.58	3.371e-3	1.60
40	3.408e-2	2.218	1.597e-3	1.79	1.376e-2	1.77	1.782e-4	1.76	9.391e-4	1.76
80	1.785e-2	2.656	3.728e-4	2.25	3.262e-3	2.23	4.255e-5	2.21	2.239e-4	2.22
160	9.061e-3	2.712	9.872e-5	1.96	8.648e-4	1.96	1.136e-5	1.95	6.002e-5	1.94
320	4.638e-3	2.832	2.511e-5	2.05	2.201e-4	2.04	2.904e-6	2.04	1.537e-5	2.03
640	2.289e-3	2.717	6.293e-6	1.96	5.527e-5	1.96	7.160e-7	1.98	3.849e-6	1.96

**The shrinking bubble problem.** We consider the Allen-Cahn equation (1.1) with  $M(\phi) \equiv 1$  and  $\varepsilon = 0.01$  in a rectangular domain  $(-0.5, 0.5)^2$ . The initial bubble is given by

$$\phi_0(\mathbf{x}) = \begin{cases} 1, & |\mathbf{x}|^2 < 0.2^2, \\ -1, & |\mathbf{x}|^2 \geq 0.2^2. \end{cases}$$

As discussed in [5, 15, 21, 32], this model describes the evolution in time of a shrinking bubble with the initial radius  $R_0 = 0.2$ , and the velocity of this circular moving interface approximately satisfies the following relation

$$R(t) = \sqrt{R_0^2 - 2\varepsilon^2 t}, \quad (5.1)$$

if  $\varepsilon$  is sufficiently small. Here,  $R(t)$  is the radius of the circle at time  $t$ .

The simulation is performed by the BDF2 scheme (2.15) with  $h = 1/512$ . The uniform time steps are used here with the time step size  $\tau = \mathcal{G}(1)/[S + 4\varepsilon^2/h^2]$ , which is the maximum value satisfying the requirement (3.8). Snapshots of the simulated bubble at the times  $t = 0, 20, 80, 120, 180, 200$  are displayed in Fig. 2, which shows that the bubble disappears at  $t = 200$

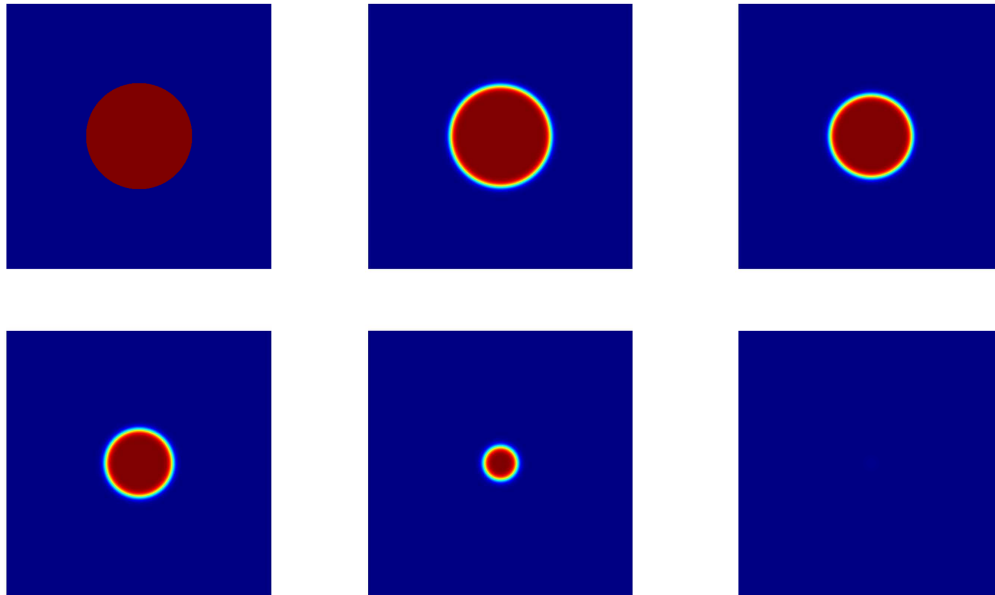


FIGURE 2. Snapshots of the simulated phase structures at the times  $t = 0, 20, 80, 120, 180,$  and  $200$  produced by the BDF2 scheme (2.15) for the shrinking bubble problem.

as expected. Moreover, we plot the evolution in time of the radius of the simulated bubble in Fig. 3-(a), which matches the prediction (5.1) very well. Several cross-section views with  $y = 0$  for the simulated solution are presented in Fig. 3-(b) and the evolution of its supremum norm along with the time is displayed in Fig. 3-(c), which demonstrate the MBP preservation of the proposed BDF2 scheme (2.15) during the whole simulation. Furthermore, it is also observed that the energy of the simulated solution is monotonically decreasing in time as shown in Fig. 3-(d).

**The grain coarsening dynamics with a time adaptive strategy.** Finally, we investigate the efficiency and the MBP preservation of the proposed BDF2 scheme (2.15) with a time adaptive strategy for the simulation of the grain coarsening. The coarsening dynamic process usually goes through several different stages within a long period: changes quickly at the beginning and then rather slowly until it reaches a steady state. In particular, we consider the coarsening dynamics governed by the Allen-Cahn equation (1.1) with the nonlinear degenerate mobility  $M(\phi) = 1 - \phi^2$  and  $\varepsilon = 0.01$ . Particularly, it is of great importance to preserve the numerical solution  $\phi \in [-1, 1]$  in the numerical algorithm for such a nonlinear mobility function. Otherwise, the numerical solutions may blow up during the time simulation.

The domain is set to be  $\Omega = (-0.5, 0.5)^2$ , and the initial value configuration is given by a randomly sampled data ranging from  $-0.9$  to  $0.9$ . There already exist several efficient time adaptive strategies [19, 41, 45, 46, 49] available to be used together with numerical schemes with variable time steps. In this simulation, we will adopt the following robust time adaptive strategy

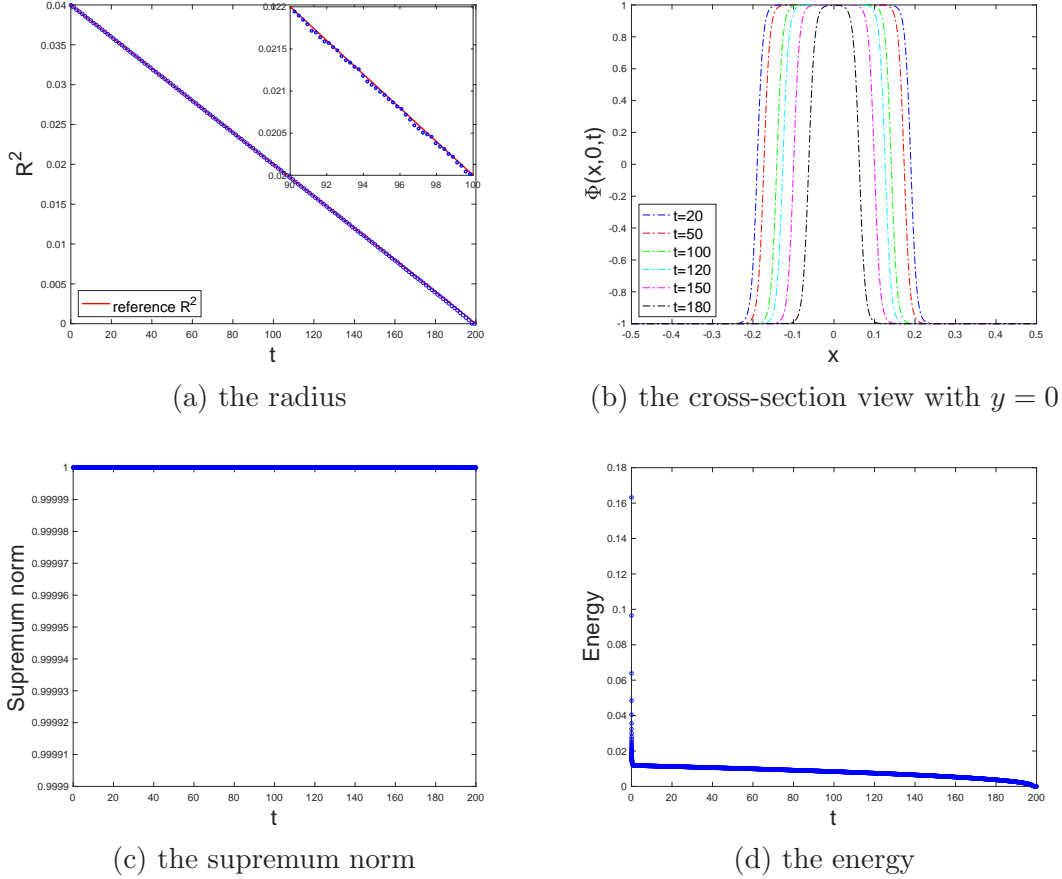


FIGURE 3. The evolutions in time of the radius, the cross section of  $y = 0$ , the supremum norm, and the energy of the simulated solution produced by the BDF2 scheme (2.15) with uniform time steps for the shrinking bubble problem.

based on the energy variation proposed in [45]:

$$\tau_{n+1} = \min \left( \max \left( \tau_{min}, \frac{\tau_{max}}{\sqrt{1 + \alpha |E'(t)|^2}} \right), \gamma_{max} \tau_n \right), \quad (5.2)$$

where  $\tau_{min}, \tau_{max}$  denote the predetermined minimum and maximum time step sizes,  $\gamma_{max} \in (0, 1 + \sqrt{2})$  is the predetermined maximum time step ratio, and  $\alpha > 0$  is a constant parameter. Such time adaptive strategy will automatically select large time steps when energy decays rapidly and small ones otherwise. We numerically solve the coarsening dynamics problem using the BDF2 scheme with four different types of temporal meshes, including the uniform time stepping with a large step size  $\tau = 0.1$ , two different ones from the time adaptive strategy (5.2), and the uniform time stepping with a small step size  $\tau = 0.01$ . For the time adaptive strategy (5.2), we always set  $\gamma_{max} = 1.5$ ,  $\alpha = 10^5$  and  $\tau_{min} = 10^{-5}$ . Also the predetermined maximum time step sizes are set to be  $\tau_{max} = \mathcal{G}(1.5)/[S + 4L\varepsilon^2/h^2] = 0.0159$  satisfying the requirement (3.8) and a large one  $\tau_{max} = 0.1$  for the two tested adaptive temporal meshes, respectively. A visual comparison on the numerical solution evolution between these four types of temporal meshes is presented in Figs. 4 and 5. It is observed that there is no obvious difference at about  $t = 10$

for the four tested temporal meshes as shown in the first line of Fig. 4, in which the snapshot of the simulated phase structure with the uniform large time step size  $\tau = 0.1$  only differs from other three temporal grids in a few small details. As shown in Figs. 4 and 5-(b), these minor phase-structure differences at  $t = 10$  gradually lead to inaccurate solution evolution and energy evolution for the case of the uniform large time step size  $\tau = 0.1$ , while the tested two adaptive time strategies still produce correct coarsening pattern which is consistent with the numerical results computed by the small time step case  $\tau = 0.01$ . In Fig. 5-(a), we successfully verify the MBP-preserving property of the BDF2 scheme by displaying the evolution of the supremum norm of the numerical solution. We also note that although both the uniform large time step case  $\tau = 0.1$  and the adaptive time strategy case with  $\tau_{max} = 0.1$  don't satisfy the condition (3.8), they still maintain the MBP-preserving property. It suggests that the constraint (3.8) on the time step size may not be optimal for the proposed BDF2 scheme (2.15) in term of preserving the discrete MBP property. Furthermore, the evolutions of the energy and the adaptive time step sizes, plotted in Fig. 5-(b)&(c), demonstrate the monotonic energy dissipation and the efficiency of the BDF2 scheme with the time adaptive strategy.

## 6. CONCLUDING REMARKS

In this paper we propose a second-order BDF scheme with nonuniform time steps for the Allen-Cahn equation with a general mobility. The MBP preservation of the proposed scheme is successfully established with mild restrictions on the time step sizes and the ratio of adjacent time step sizes. Moreover, the discrete  $H^1$  error estimate and energy stability are rigorously derived for the constant mobility case and so does the  $L^\infty$  error estimate for the general mobility case. Finally, various numerical experiments are carried out to validate the theoretical results and demonstrate the performance of the proposed scheme adopted with a time adaptive strategy. It remains interest to further theoretically explore the discrete  $H^1$  error analysis and energy stability for the general mobility case, and study the Allen-Cahn equation with the logarithmic potential, instead of the double-well potential studied in this paper. Moreover, we also would like extend the present work to the time-fractional Allen-Cahn equation, in which it is urgently desired to make use of variable-step structure-preserving high-order time stepping schemes to overcome the initial singularity from fractional derivatives. In addition, there are two non-constant coefficient Poisson-type equations to be solved at each time step for the model with non-constant mobility in the proposed linear BDF2 scheme. Consequently, it may not be computationally cheaper and more accurate than a comparable second-order nonlinear scheme with the use of nonlinear multigrid method [8, 53]. Thus, it is also an interesting future work to study nonlinear MBP-preserving numerical schemes for the Allen-Cahn equation with variable mobility.

## REFERENCES

- [1] G. Akrivis, B. Li, and D. Li. Energy-decaying extrapolated RK-SAV methods for the Allen-Cahn and Cahn-Hilliard equations. *SIAM J. Sci. Comput.*, 41(6):A3703–A3727, 2019.
- [2] A. Baskaran, Z. Hu, J. S. Lowengrub, C. Wang, S. M. Wise, and P. Zhou. Energy stable and efficient finite-difference nonlinear multigrid schemes for the modified phase field crystal equation. *J. Comput. Phys.*, 250:270–292, 2013.

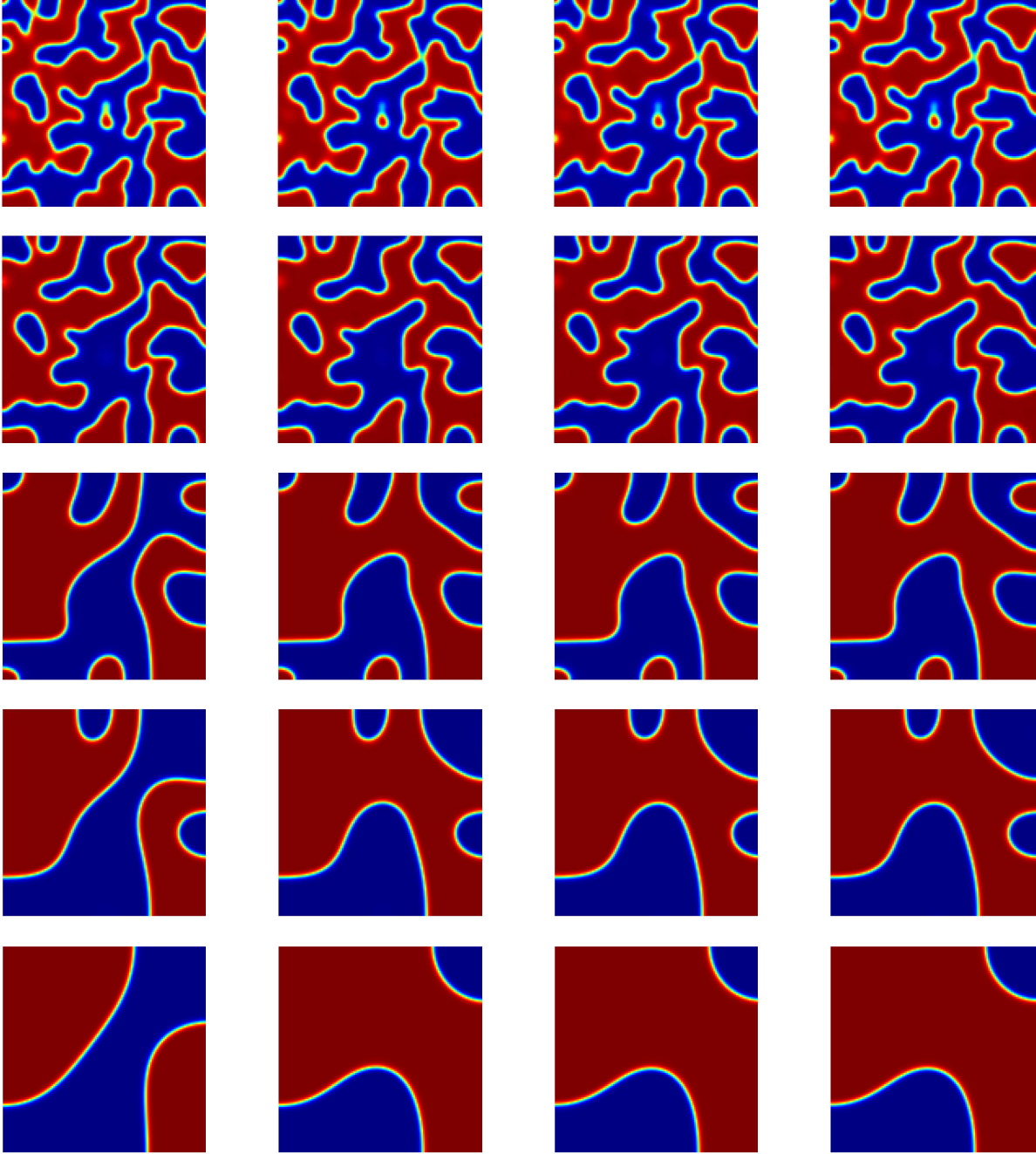


FIGURE 4. Snapshots of the simulated phase structures around the times  $t = 10$ , 20, 100, 200, and 500 from top to bottom produced by the BDF2 scheme (2.15) with  $h = 1/128$  and four tested temporal meshes: the uniform time stepping with fixed large time step size  $\tau = 0.1$  (the first column); the time adaptive strategy (5.2) with  $\tau_{max} = 0.1$  (the second column); the time adaptive strategy (5.2) with  $\tau_{max} = \mathcal{G}(1.5)/[S + 4L\epsilon^2/h^2]$  (the third column); the uniform time stepping with fixed small time step size  $\tau = 0.01$  (the last column).



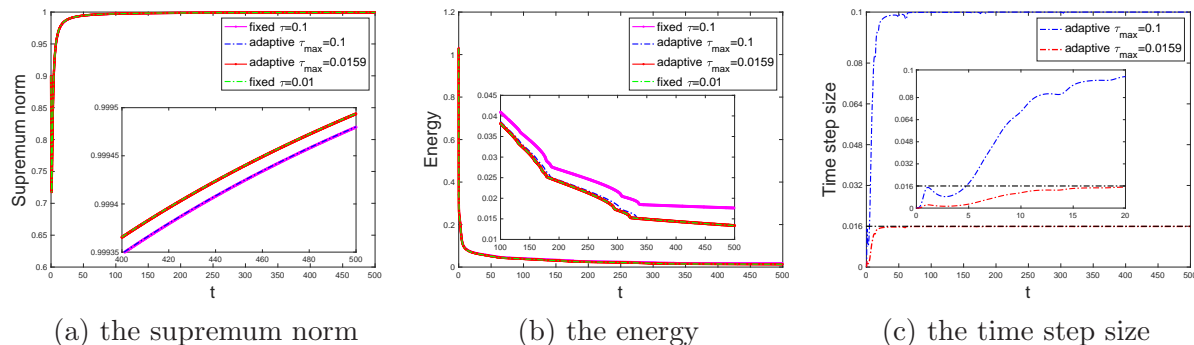


FIGURE 5. The evolutions in time of the supremum norm, the energy, and the time step sizes produced by the BDF2 scheme (2.15) with four types of temporal meshes for the grain coarsening problem.

- [3] A. Baskaran, J. S. Lowengrub, C. Wang, and S. M. Wise. Convergence analysis of a second order convex splitting scheme for the modified phase field crystal equation. *SIAM J. Numer. Anal.*, 51(5):2851–2873, 2013.
- [4] J. Becker. A second order backward difference method with variable steps for a parabolic problem. *BIT*, 38(4):644–662, 1998.
- [5] L. Chen and J. Shen. Applications of semi-implicit fourier-spectral method to phase field equations. *Comput. Phys. Commun.*, 108(2-3):147–158, 1998.
- [6] W. Chen, S. Conde, C. Wang, X. Wang, and S. M Wise. A linear energy stable scheme for a thin film model without slope selection. *J. Sci. Comput.*, 52(3):546–562, 2012.
- [7] W. Chen, W. Li, Z. Luo, C. Wang, and X. Wang. A stabilized second order exponential time differencing multistep method for thin film growth model without slope selection. *ESAIM Math. Model. Numer. Anal.*, 54(3):727–750, 2020.
- [8] W. Chen, C. Wang, X. Wang, and S. M Wise. Positivity-preserving, energy stable numerical schemes for the cahn-hilliard equation with logarithmic potential. *J. Comput. Phys. X*, 3:100031, 2019.
- [9] W. Chen, X. Wang, Y. Yan, and Z. Zhang. A second order BDF numerical scheme with variable steps for the Cahn–Hilliard equation. *SIAM J. Numer. Anal.*, 57(1):495–525, 2019.
- [10] K. Cheng, W. Feng, C. Wang, and S. M Wise. An energy stable fourth order finite difference scheme for the Cahn–Hilliard equation. *J. Comput. Appl. Math.*, 362:574–595, 2019.
- [11] K. Cheng, Z. Qiao, and C. Wang. A third order exponential time differencing numerical scheme for no-slope-selection epitaxial thin film model with energy stability. *J. Sci. Comput.*, 81:154–185, 2019.
- [12] K. Cheng, C. Wang, S. M Wise, and Y. Wu. A third order accurate in time, BDF-type energy stable scheme for the Cahn-Hilliard equation. *Numer. Math. Theor. Meth. Appl.*, 15(2):279–303, 2021.
- [13] Q. Cheng and J. Shen. A new Lagrange multiplier approach for constructing structure preserving schemes, I. positivity preserving. *Comput. Methods Appl. Mech. Eng.*, 391:114585, 2022.

- [14] Q. Cheng and J. Shen. A new Lagrange multiplier approach for constructing structure preserving schemes, II. bound preserving. *SIAM J. Numer. Anal.*, 60(3):970–998, 2022.
- [15] J. M. Church, Z. Guo, P. K. Jimack, A. Madzvamuse, K. Promislow, B. Wetton, S. M. Wise, and F. Yang. High accuracy benchmark problems for Allen-Cahn and Cahn-Hilliard dynamics. *Commun. Comput. Phys.*, 26(4), 2019.
- [16] Q. Du, L. Ju, X. Li, and Z. Qiao. Maximum principle preserving exponential time differencing schemes for the nonlocal Allen–Cahn equation. *SIAM J. Numer. Anal.*, 57(2):875–898, 2019.
- [17] Q. Du, L. Ju, X. Li, and Z. Qiao. Maximum bound principles for a class of semilinear parabolic equations and exponential time differencing schemes. *SIAM Rev.*, 63(2):317–359, 2021.
- [18] Z. Fu and J. Yang. Energy-decreasing exponential time differencing Runge–Kutta methods for phase-field models. *J. Comput. Phys.*, 454:110943, 2022.
- [19] H. Gomez and T. JR Hughes. Provably unconditionally stable, second-order time-accurate, mixed variational methods for phase-field models. *J. Comput. Phys.*, 230(13):5310–5327, 2011.
- [20] Y. Hao, Q. Huang, and C. Wang. A third order bdf energy stable linear scheme for the no-slope-selection thin film model. *Commun. Comput. Phys.*, 29(3), 2021.
- [21] D. Hou, M. Azaiez, and C. Xu. A variant of scalar auxiliary variable approaches for gradient flows. *J. Comput. Phys.*, 395:307–332, 2019.
- [22] D. Hou and Z. Qiao. A linear adaptive BDF2 scheme for phase field crystal equation. *arXiv:2206.07625*, pages 1–21, 2022.
- [23] D. Hou and Z. Qiao. An implicit–explicit second–order BDF numerical scheme with variable steps for gradient flows. *J. Sci. Comput.*, 94(2):39, 2023.
- [24] D. Hou and C. Xu. A second order energy dissipative schemes for time fractional  $L^2$  gradient flows using SAV approach. *J. Sci. Comput.*, 90(1):25, 2022.
- [25] T. Hou and H. Leng. Numerical analysis of a stabilized Crank–Nicolson/Adams–Bashforth finite difference scheme for Allen–Cahn equations. *Appl. Math. Lett.*, 102:106150, 2020.
- [26] T. Hou, T. Tang, and J. Yang. Numerical analysis of fully discretized Crank–Nicolson scheme for fractional-in-space Allen–Cahn equations. *J. Sci. Comput.*, 72(3):1214–1231, 2017.
- [27] Z. Hu, S. M. Wise, C. Wang, and J. S. Lowengrub. Stable and efficient finite-difference nonlinear-multigrid schemes for the phase field crystal equation. *J. Comput. Phys.*, 228(15):5323–5339, 2009.
- [28] K. Jiang, L. Ju, J. Li, and X. Li. Unconditionally stable exponential time differencing schemes for the mass-conserving Allen–Cahn equation with nonlocal and local effects. *Numer. Methods Partial Differ. Equ.*, 38(6):1636–1657, 2022.
- [29] L. Ju, X. Li, and Z. Qiao. Generalized SAV–exponential integrator schemes for Allen–Cahn type gradient flows. *SIAM J. Numer. Anal.*, 60(4):1905–1931, 2022.
- [30] L. Ju, X. Li, and Z. Qiao. Stabilized exponential–SAV schemes preserving energy dissipation law and maximum bound principle for the Allen–Cahn type equations. *J. Sci. Comput.*, 92(2):66, 2022.
- [31] L. Ju, X. Li, Z. Qiao, and J. Yang. Maximum bound principle preserving integrating factor Runge–Kutta methods for semilinear parabolic equations. *J. Comput. Phys.*, 439:110405, 2021.

- [32] L. Ju, J. Zhang, L. Zhu, and Q. Du. Fast explicit integration factor methods for semilinear parabolic equations. *J. Sci. Comput.*, 62(2):431–455, 2015.
- [33] B. Li, J. Yang, and Z. Zhou. Arbitrarily high-order exponential cut-off methods for preserving maximum principle of parabolic equations. *SIAM J. Sci. Comput.*, 42(6):A3957–A3978, 2020.
- [34] J. Li, L. Ju, Y. Cai, and X. Feng. Unconditionally maximum bound principle preserving linear schemes for the conservative Allen–Cahn equation with nonlocal constraint. *J. Sci. Comput.*, 87(3):1–32, 2021.
- [35] J. Li, X. Li, L. Ju, and X. Feng. Stabilized integrating factor Runge–Kutta method and unconditional preservation of maximum bound principle. *SIAM J. Sci. Comput.*, 43(3):A1780–A1802, 2021.
- [36] W. Li, W. Chen, C. Wang, Y. Yan, and R. He. A second order energy stable linear scheme for a thin film model without slope selection. *J. Sci. Comput.*, 76:1905–1937, 2018.
- [37] X. Li, Z. Qiao, and C. Wang. Convergence analysis for a stabilized linear semi-implicit numerical scheme for the nonlocal Cahn–Hilliard equation. *Math. Comput.*, 90(327):171–188, 2021.
- [38] X. Li, J. Shen, and H. Rui. Energy stability and convergence of SAV block-centered finite difference method for gradient flows. *Math. Comput.*, 88(319):2047–2068, 2019.
- [39] H. Liao, B. Ji, L. Wang, and Z. Zhang. Mesh-robustness of an energy stable BDF2 scheme with variable steps for the Cahn–Hilliard model. *J. Sci. Comput.*, 92(2):52, 2022.
- [40] H. Liao, W. McLean, and J. Zhang. A discrete Gronwall inequality with applications to numerical schemes for subdiffusion problems. *SIAM J. Numer. Anal.*, 57(1):218–237, 2019.
- [41] H. Liao, T. Tang, and T. Zhou. On energy stable, maximum-principle preserving, second order BDF scheme with variable steps for the Allen–Cahn equation. *SIAM J. Numer. Anal.*, 58(4):2294–2314, 2020.
- [42] H. Liao and Z. Zhang. Analysis of adaptive BDF2 scheme for diffusion equations. *Math. Comput.*, 90:1207–1226, 2020.
- [43] C. Lv and C. Xu. Error analysis of a high order method for time-fractional diffusion equations. *SIAM J. Sci. Comput.*, 38(5):A2699–A2724, 2016.
- [44] X. Meng, Z. Qiao, C. Wang, and Z. Zhang. Artificial regularization parameter analysis for the no-slope-selection epitaxial thin film model. *CSIAM Trans. Appl. Math.*, 1(3):441–462, 2020.
- [45] Z. Qiao, Z. Zhang, and T. Tang. An adaptive time-stepping strategy for the molecular beam epitaxy models. *SIAM J. Sci. Comput.*, 33(3):1395–1414, 2011.
- [46] J. Shen, T. Tang, and J. Yang. On the maximum principle preserving schemes for the generalized Allen–Cahn equation. *Commun. Math. Sci.*, 14(6):1517–1534, 2016.
- [47] J. Shen, C. Wang, X. Wang, and S. M. Wise. Second-order convex splitting schemes for gradient flows with Ehrlich–Schwoebel type energy: application to thin film epitaxy. *SIAM J. Numer. Anal.*, 50(1):105–125, 2012.
- [48] J. Shen, J. Xu, and J. Yang. The scalar auxiliary variable (SAV) approach for gradient flows. *J. Comput. Phys.*, 353:407–416, 2018.
- [49] J. Shen, J. Xu, and J. Yang. A new class of efficient and robust energy stable schemes for gradient flows. *SIAM Rev.*, 61(3):474–506, 2019.
- [50] T. Tang and J. Yang. Implicit–explicit scheme for the Allen–Cahn equation preserves the maximum principle. *J. Comput. Math.*, 34(5):451–461, 2016.

- [51] A. Weiser and M. F. Wheeler. On convergence of block-centered finite differences for elliptic problems. *SIAM J. Numer. Anal.*, 25(2):351–375, 1988.
- [52] S. M Wise. Unconditionally stable finite difference, nonlinear multigrid simulation of the Cahn-Hilliard-Hele-Shaw system of equations. *J. Sci. Comput.*, 44(1):38–68, 2010.
- [53] S. M Wise. Unconditionally stable finite difference, nonlinear multigrid simulation of the Cahn-Hilliard-Hele-Shaw system of equations. *J. Sci. Comput.*, 44(1):38–68, 2010.
- [54] S. M. Wise, C. Wang, and J. S. Lowengrub. An energy-stable and convergence finite-difference scheme for the phase field crystal equation. *SIAM J. Numer. Anal.*, 47(1):2269–2288, 2009.
- [55] Y. Yan, W. Chen, C. Wang, and S. M Wise. A second-order energy stable BDF numerical scheme for the Cahn-Hilliard equation. *Commun. Comput. Phys.*, 23(2):572–602, 2018.
- [56] J. Yang, Z. Yuan, and Z. Zhou. Arbitrarily high-order maximum bound preserving schemes with cut-off postprocessing for Allen–Cahn equations. *J. Sci. Comput.*, 90(2):1–36, 2022.
- [57] H. Zhang, J. Yan, X. Qian, X. Gu, and S. Song. On the maximum principle preserving and energy stability of high-order implicit-explicit Runge-Kutta schemes for the space-fractional Allen-Cahn equation. *Numer. Algor.*, 88:1309–1336, 2021.
- [58] H. Zhang, J. Yan, X. Qian, and S. Song. Numerical analysis and applications of explicit high order maximum principle preserving integrating factor Runge-Kutta schemes for Allen–Cahn equation. *Appl. Numer. Math.*, 161:372–390, 2021.